Available online at www.sciencedirect.com
ScienceDirect
Geomorphology 86 (2007) 369–392
GEOMORPHOLOGY
www.elsevier.com/locate/geomorph

Origin of the sedimentary deposits of the Naracoorte Caves, South Australia

M.S. Forbes *, E.A. Bestland [1]

School of Chemistry, Physics and Earth Sciences, Flinders University SA, GPO Box 2100, Adelaide, South Australia 5162, Australia

Received 5 June 2006; received in revised form 9 September 2006; accepted 12 September 2006
Available online 30 October 2006

Abstract

The origin of the sediments located in the Naracoorte Caves (South Australia) was investigated via the analysis of strontium isotope ratios ($^{87}Sr/^{86}Sr$), elemental geochemistry, and mineralogy. Sedimentary deposits located in Robertson, Wet, Blanche and several other chambers in Victoria Cave are all variable mixes of fine sand and coarse silts, which display similar and consistent strontium isotope ratios (0.717–0.725). This suggests that over the 400 ka time frame that these deposits span there has been minimal variation in the source of the clastic sediments. Increased strontium concentrations for these cave sediments correspond with increasing silt content, yet there is no correlation between $^{87}Sr/^{86}Sr$ ratios and silt content. This implies that the silt-sized component of the sediments is the main contributor of strontium to the cave sediments. Comparisons of $^{87}Sr/^{86}Sr$ with regional surficial deposits show a significant correlation between the cave sediments (avg: 0.7228; $n=27$), the fine silt lunettes of the Bool Lagoon area (avg: 0.7224; $n=4$), the sandy A horizons of the Coonawarra Red Brown Earths (RBEs; avg: 0.726; $n=5$), and Holocene age podsolic sand deposits (0.723). These data suggest that there has been substantial flux from this group of deposits to the caves, as would be expected considering prevailing winds. This relationship is further supported by a strong correlation between many trace elements, including Ti, Zr, Ce, and Y; however, variations in clay mineralogy suggest that the fine silt-dominated lunettes and Padthaway RBEs were not significant contributors to the cave deposits. Hence, the detritus entering the caves was more than likely from areas proximal to the cave entrance and was dominated by medium grain-sized materials. Major regional deposits, including the coarser-grained, calcite-rich Bridgewater Formation sands, basalts from the lower SE, Padthaway Horst granites, Gambier limestone, and metamorphics from the Adelaide geosyncline show minimal correlation in $^{87}Sr/^{86}Sr$ ratios, elemental geochemistry, and mineralogy with the cave sediments, and are discounted as significant sources. In comparison, $^{87}Sr/^{86}Sr$ ratios for the Coorong silty sands (0.717–0.724), Lower Murray sands (0.727–0.730), and the medium size silt component of the Murray–Darling River system (0.71–0.72), compare favourably with the cave sediments. This relationship is further supported by similarities in elemental chemistry and mineralogy. Thus, much of the strontium-rich silt that is now located in the Naracoorte Cave sediments likely originated from the Murray–Darling basin. Over time, this material has been transported to the SE of South Australia, where it mixed with the medium sand component of the regressive dune ridge sequence, locally derived organic matter, limestone fragments, and fossil material to produce the unique deposits that we see evident in many of the chambers of the Naracoorte Cave system today.

Keywords: Naracoorte Cave sediments; South Australia; Strontium isotopes; Murray basin; Geochemistry; Mineralogy

* Corresponding author. Current address: CSIRO Land and Water, PMB 2 Glen Osmond, South Australia, Australia 5062. Tel.: +61 8 8303 8512; fax: +61 8 8303 8550.
E-mail addresses: matthew.forbes@csiro.au (M.S. Forbes), erick.bestland@flinders.edu.au (E.A. Bestland).
[1] Tel.: +61 8 8201 2306; fax: +61 8 8201 2676.

0169-555X/$ - see front matter © 2006 Elsevier B.V. All rights reserved.
doi:10.1016/j.geomorph.2006.09.009

1. Introduction

The origin of the sedimentary accumulations that now fill the chambers of the World Heritage Naracoorte Caves has been of interest to researchers since the late 1960s discovery of fossil vertebrates in Victoria Cave. During numerous palaeontological studies, a connection between cave sediments and several of the area's surficial deposits has been made, linked by distinct similarities in sedimentary physical characteristics and the numerous dolines and bedrock collapse sink holes that litter the region (Wells et al., 1984; Brown and Wells, 2000; Moriarty et al., 2000; McDowell, 2001). Sand-rich horizons, which dominate many of the cave deposits, have been related to the region's regressive dune sequences (Wells et al., 1984); while the red silt horizons, also prevalent in numerous of the cave deposits are thought to be eroded components of the area's famous Red Brown Earths (RBEs) or Terra Rossa soils (Moriarty et al., 2000; McDowell, 2001). The Gambier limestone host-rock has also been recognised as a contributor to the composition of the cave fills, via the identification of weathered fragments amongst many of the sediment accumulations. As yet, no geochemical data to confirm any of these relationships exists; rather, geochemical research has been focussed on determining the age of fossil accumulations via the analysis of calcite deposits (Ayliffe and Veeh, 1988; Moriarty et al., 2000; Grün et al., 2001) and charcoal fragments (McDowell, 2001; Pate et al., 2002), as well as palaeoenvironmental interpretations derived from speleothems (Desmarchelier et al., 2000).

Strontium isotope ratios ($^{87}Sr/^{86}Sr$), as well as the mineralogical, and elemental composition of the cave sediments and regional surficial deposits are presented in this study. Comparisons of this data set to those determined for the region (including local surficial deposits, the Adelaide geosyncline, Murray Basin, and to a lesser extent central Australia) will lead to a more quantitative and thus significantly better appreciation of the origin of the cave fills.

The analysis of $^{87}Sr/^{86}Sr$ ratios to trace the source of surficial sediments is extensive (e.g., Faure and Powell, 1972; Capo et al., 1998; Stewart et al., 1998). This is because strontium is widespread in the natural environment and because the $^{87}Sr/^{86}Sr$ ratio of components of the sedimentary system varies depending on the strontium's original geological source. Although $^{87}Sr/^{86}Sr$ ratio analysis of clastic cave sediments have in the past proved effective in characterising Quaternary soil erosion rates (Cooke et al., 2003), $^{87}Sr/^{86}Sr$ applications to cave research has been predominantly focussed on palaeoenvironmnetal studies of speleothems (e.g., Goede et al., 1998; Ayalon et al., 1999; Frumkin and Stein, 2004).

In comparison, the mineralogical identification and quantification of cave sediments via X-ray diffraction (XRD) is well established (e.g., Ford and Williams, 1989; Hill and Forti, 1997; Karkanas et al., 1999; Shahack-Gross et al., 2004; Zanin et al., 2005). Quantitative mineralogy can provide a sound understanding of cave sediment evolution because many of the minerals found in cave deposits reflect the conditions and sediment types that existed during the minerals formation. Hence, the dominant geochemical processes (either inside or outside the cave environment) can be identified, allowing for insights into the sediment's origin.

The use of bulk sediment geochemistry (XRF) is common in the understanding of soil forming processes, including the identification of critical components of a soil system (e.g., Zr, P, B, Ti, Y, and Ce) that have remained unaltered and immobile since its inception. Such components are particularly effective in tracing the origins of many soil and sediment accumulations (e.g., Dickson and Scott, 1998; Fitzpatrick and Chittleborough, 2002). For example, investigations of Ti/Zr ratios have proven useful in recognising aeolian contributions to soils (Dickson and Scott, 1998). While these geochemical methods have yet to be applied directly to the sediments in the Naracoorte Caves, they have been used effectively in studies regarding the origins and soil properties of the region's RBEs (Green et al., 2004; Mee et al., 2004; Krull et al., 2006). Mee et al. (2004) investigated $^{87}Sr/^{86}Sr$ ratios, mineralogy, and bulk sediment chemistry of RBEs from the Coonawarra area (identifying aeolian-derived materials) rather than products from limestone dissolution as the major contributor to their formation. $^{87}Sr/^{86}Sr$ analysis has also been undertaken on many geological and sedimentary deposits in southern Australia (e.g., Turner et al., 1993; Douglas et al., 1995; Quade et al., 1995; Price et al., 1997; Dogramaci and Herczeg, 2002). Mineralogical analysis and bulk rock and sediment elemental analysis have also been carried out on many of the regional surficial deposits (e.g., Norrish and Rogers, 1956; Turner et al., 1993; Douglas et al., 1995; Gingele et al., 2004). The objective of this study is to understand the origin and evolutionary history of the clastic materials that now fill the cave system. This will be achieved via comparisons of $^{87}Sr/^{86}Sr$ data, mineralogical and bulk sediment geochemistry for the Naracoorte Cave sediments, the surficial deposits of the surrounding region and the greater southeastern region of Australia.

2. Regional setting

2.1. Geological setting

The Naracoorte Caves system developed during the Late Miocene/Pliocene in the Oligo-Miocene Gambier limestone that underlies much of SE South Australia (Fig. 1). The cave system follows the extreme western edge of an uplifted limestone plateau adjacent to the Kanawinka Fault (Sprigg, 1952), with their formation controlled by a combination of structural and hydrological influences (Wells et al., 1984; White, 2005). The earlier movement of the Kanawinka Fault flexed the limestone base and thus determined the joint directions (north-northwest and east-northeast) and distribution, while the position of the sea level controlled the configuration of the water table and groundwater flow directions. As sea level dropped throughout the Pleistocene the regional water table fell, allowing the caves to drain. The majority of the cave fills are situated in this uplifted portion of the phreatic karst and have been in the vadose zone since the late Early Pleistocene (Moriarty et al., 2000). As a result, they have been largely unaffected by regional stream flows. This limestone is now overlain by a succession of 13 stranded beach–dune ridges that stretch from Naracoorte in the east to Robe in the west (Sprigg, 1952, 1979; Cook et al., 1977; Twidale et al., 1983). This Plio–Pleistocene sequence (known as the Bridgewater Formation) formed as a result of several sea-level transgression–regression cycles and crustal uplift. It now covers the older phreatic caverns, thus protecting them from erosion. Other regional sand units that are also currently present on the uplifted limestone area include the Pliocene Parilla Sands and the Holocene podsolic sands, these sandwich the Bridgewater Formation chronologically (Twidale et al., 1983).

Located between these NNW–SSE-trending relict beach–dune ridges are flat, typically poorly drained areas dominated by small to medium-sized playas, lagoons, and swamps. Boarded on the eastern (leeward) side of many of these seasonal water features are low crescent ridges or lunettes. The lunettes formed as a result of deflation and reworking of the lakebed material during dry seasons (Twidale et al., 1983) and display scattered cross-bedding that is consistent with aeolian deposition (Bowler et al., 1976). Another significant surficial deposit in the Naracoorte region is the Terra Rossa soils or Red Brown Earths (RBEs). These soils typically consist of a sandy A horizon and a heavy red clay B horizon situated over a calcarenite or limestone base (Blackburn et al., 1965; Stace et al., 1968; Mee et al., 2004; Krull et al., 2006). These surficial sediments are thought to have been eroded and deposited into the cave chambers intermittently since the mid-Pleistocene (Wells et al., 1984; Moriarty et al., 2000; McDowell, 2001).

2.2. Cave sediments

Six sedimentary accumulations situated in the four caves around Naracoorte were the focus of this study. They include Robertson Cave, Wet Cave, Blanche Cave, and the extensive Victoria Cave, which is comprised of several separate chambers: Starburst Chamber, Grant Hall, and the main Fossil Chamber. All have had significant palaeontological and chronological research previously undertaken on them (e.g., Wells et al., 1984; Moriarty et al., 2000; McDowell, 2001; Reed, 2002). The application of various dating techniques has intermittently placed the above-mentioned group of cave deposits between 400 ka to present. Thermal ionisation mass spectrometry (TIMS) and U-series dating (Ayliffe and Veeh, 1988; Ayliffe et al., 1998) coupled with electron spin resonance (ESR) dating of flowstones (Grün et al., 2001), which sandwich the clastic and fossiliferous sediments, has identified an age bracket of 125 to 500 ka for the three deposits located in Victoria Cave. These include 280–500 ka for the accumulation in the Victoria Cave Fossil Chamber, >125 ka for Grant Hall and 190–350 ka for Starburst Chamber. The age of the younger Late Pleistocene to Holocene sediment fills of Robertson, Wet, and Blanche Caves were determined via radiocarbon dating of charcoal fragments extracted from numerous sedimentary horizons. Results indicate that the Robertson Cave sediments span from >32 to 8 ka (McDowell, 2001) and the Wet Cave accumulation covers 45 ka and 800 yr (McDowell, 2001; Pate et al., 2002), while two unpublished ^{14}C dates for the Blanche Cave sediments indicate and age range of 11 to 13 ka.

Sediments, bones, and water access into the chambers of Victoria Cave have generally been restricted to small, shallow dolines of 3 to 150 m in diameter on the ridge top (Wells et al., 1984). In comparison, sediment access into Robertson, Wet, and Blanche caves has been via more open collapsed roof entrances (McDowell, 2001). For all deposits, minor runoff flows have dominated the bulk of clastic sediment transport into the caverns, over time these accumulations formed large talus cones beneath the entrance points to the caves (Wells et al., 1984). This process has then been followed by erosion and reworking of the sediment talus cones transporting the sediments farther into the cave system.

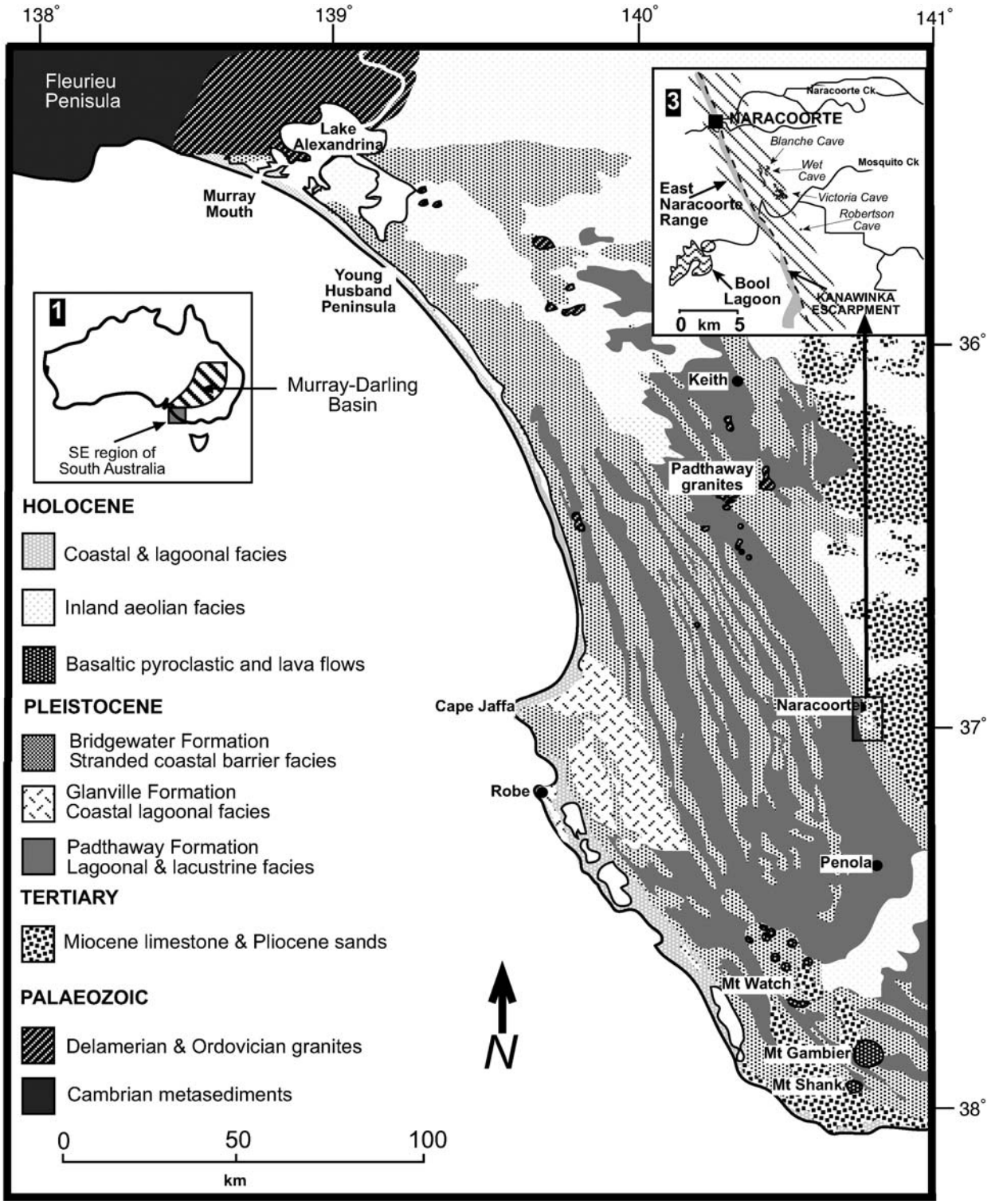

Fig. 1. Regional map of South Australia, focussing on the SE and the location of the Naracoorte Caves, and the various sedimentary deposits of the region.

The physical characterisation of the six sedimentary deposits was undertaken in the past primarily as part of broader palaeontological studies (e.g., Wells et al., 1984; Moriarty et al., 2000; McDowell, 2001; Reed, 2002). Identified in all six accumulations were variable distributions of three dominant horizon types: homogeneous yellowish sands, reddish sandy silts, and brown organic matter rich sandy silts. In the Victoria Fossil Chamber, a dominance by siliceous sands is apparent (Moriarty et al., 2000; Reed, 2002), with variations in texture and colour between sediment horizons being attributed to differences in clay and clast content rather than sorting of sand grain sizes. The clasts consist of limestone, clay, calcrete, bone, and occasional pieces of speleothem; while the clays occur mainly in the rounded silt- to sand-sized particles. Various amounts of different sized charcoal fragments are also evident within these deposits. Sediments excavated from the 1-m-thick fan in the Starburst Chamber are comprised of yellow–orange quartz sand and red–brown clayey sand (Moriarty et al., 2000). These sediments include sparse clasts of calcrete, limestone, and bone, interpreted as infall debris that was washed from the cone onto the accumulating fan. In Grant Hall, a 1-m-thick low-angle fan has also been excavated and consists predominantly of very dark reddish brown clayey sands with abundant pebble-sized clasts of weathered limestone, calcrete, charcoal, and bone. These clastic deposits are capped by a clean laminated flowstone and underlain by stalagmite-covered limestone (Moriarty et al., 2000). Investigations of the interior fan deposit in Robertson (McDowell, 2001, Forbes et al., in press) and Blanche Caves (Steve Brown, Flinders University, personal communication, 2004) and the semi-entrance facies in Wet Cave (McDowell, 2001) identified a similar sedimentary record for all three. These deposits (in particular those located in Robertson and Wet Caves) contain older red silts overlain by yellow sands that are, in turn, capped by darker, organic-rich silts and sands. The latter is clearly absent from the Victoria Cave chambers. The darker, organic-rich sediments are thought to be eroded modern solum or podsolic sands that developed in the region during the Late Pleistocene and Holocene (McDowell, 2001). Various clasts of weathered limestone, calcrete, charcoal, and bone are found throughout the three deposits; and the fan deposit in Blanche Cave is capped by a laminar flowstone.

3. Materials and methods

3.1. Strontium isotopes

Samples for $^{87}Sr/^{86}Sr$ isotope analysis were prepared and analysed at the school of Earth and Environmental Sciences, Adelaide University. Sample weights of between 0.1 to 0.2 g of milled sediment were placed in Teflon beakers that had been boiled in 6 M HNO_3, 6 M HCl, and deionised (DI) water, with each being rinsed three times with DI water between treatments. Subsequently, 4 ml of 50% HF was then added to the samples and heated to 150 °C overnight to dissolve any silicate materials present. Each sample was heated until total evaporation occurred; however, just prior to complete dryness, 1 ml 6 M HNO_3 was added to prevent insoluble fluorides forming. Then 4 ml HF and 1 ml 6 M HNO_3 was again added to each sample and then heat-treated for 2 d, with samples again having 1 ml 6 M HNO_3 added just prior to being evaporated to dryness. Next 1 ml 6 M HCl was added to the rock samples. They were heated overnight to dryness and then redissolved in 1.5 ml 2 M HCl. Each sample was then centrifuged for 5 min at 3000 rpm, with 1 ml of the resulting supernatant passed through a cation exchange resin with HCl as the eluent. The elution was evaporated to dryness, then reconstituted in 1 ml 2 M HCl and passed through a second time to ensure as much ^{87}Rb as possible was removed from the elution. This is required as any residual ^{87}Rb in the sample would complicate the analysis of the mass spectrometer $^{87}Sr/^{86}Sr$ measurements. Samples are once again evaporated to dryness and the purified Sr is reconstituted in 2 μl of Birck® Solution (Paris, composed primarily of TaO, plus HF, HNO_3, and H_3PO_4) and loaded onto a single Ta (tantalum) filament using the sandwich technique for mass spectrometric measurement. The isotopic composition of Sr (IC) was measured on a Finnigan MAT® 262 thermal ionisation mass spectrometer (TIMS). Final results were normalised to the expected standard 0.710248 using replicate measurements of the standards NBS SRM 987-189 to 193.

3.2. Sediment mineralogy (XRD)

Each sample was sieved with the portion of ≤212 μm being retained and crushed to a fine powder. Then, 10 g approximately of this material was shaken with 10 ml of sodium hexa-metaphosphate for 10 min before transferring into 500 ml measuring cylinders with deionised water. The suspensions were allowed to settle for 16 h, and the supernatant from a depth of 20 cm was collected (i.e., <2 μm fraction). These suspensions were flocculated with excess NaCl, centrifuged, then washed with DI water before calcium saturation (using 1 M $CaCl_2$). The <2 μm fractions were washed with DI water followed by ethanol and oven-dried at 60 °C for several hours. Each sample was then ground to an ultrafine powder in an agate mortar and pestle with 100 mg approximately then being lightly pressed into an aluminium sample holder for X-ray diffraction (XRD)

analysis. XRD patterns were recorded with a Philips PW1800 microprocessor-controlled diffractometer using Co Kα radiation, variable divergence slit, and graphite monochromator. The pressed powder diffraction patterns were recorded from 3° to 80° 2θ in steps of 0.05°, 3.0-s counting time per step, and logged to data files for analysis. Quantitative analysis was undertaken on the <2 μm fractions using the commercial package SIROQUANT, with the data being background subtracted and calibrated for the use of the variable divergence slit.

3.3. Major and trace element geochemistry (XRF)

Major elements in their oxidised state (such as SiO_2, Al_2O_3, Fe_2O_3, MnO, MgO, CaO, Na_2O, K_2O, TiO_2, P_2O_5, and SO_3) were determined as a percentage composition (Norrish and Chappell, 1977). Samples for major elemental analysis were crushed, dried at 110 °C, then combusted at 960 °C overnight, in order to determine the Loss of Ignition (LOI), which is indicative of the organic matter and hydrated mineral phases present in the sediment (Craft et al., 1991). The next day, between 1.0 and 1.1 g of the combusted material was weighed and combined with flux (35.3% lithium tetraborate and 64.7% lithium metaborate). Then, using Pt–Au crucibles the mixture was fused at 1150 °C approximately. Samples were analysed at Adelaide University using a Phillips PW 1480 XRF Spectrometer, and results are presented in their oxidised state. Minor or trace element (Sr, Rb, Y, Zr, Nb, Pb, Th, U, Ba, Sc, Ga, V, Cr, Ce, Nd, La, Ni, Cu, Zn, and Co) analysis was undertaken to obtain data in concentrations of one to several thousand parts per million (ppm).

4. Results

4.1. Physical properties of cave sediments

Sample descriptions including quantitative grain size distributions are presented in Table 1. All horizons present in the six sedimentary deposits are categorised into three general horizon types, the yellow to grey homogeneous sands (type I), the dark brown to brown organic matter rich sandy silts (type II), and the reddish brown sandy silts (type III). Grain size analysis of these sediments indicates that all three horizon types are dominated by medium and fine sands to coarse silt, with some slight variances between them. The yellow and grey homogeneous sands contain the largest medium to fine sand component of the three horizon types, while the dark brown to brown sandy silts possess a greater fine sand to coarse silt component and less medium-sized sand. The reddish sandy silts contain the most

Table 1
Naracoorte cave sediments sample description, location, and grain size distribution

Sample	Location	Description	>C. Sand	M. Sand to F. Sand	V.F. Sand to C. Silt	<C. Silt
			mm (>0.5)	(0.5 to 0.3)	(0.3 to 0.1)	<0.1
Robertson Cave						
R 0	Robertson Cave Pit 1 65 cm	10 YR dark brown silt	5.3	10.3	44.9	39.5
R 6	Robertson Cave Pit 1 120 cm	10 YR dark brown sandy silt	3.4	25.3	50.9	20.5
R 12	Robertson Cave Pit 1 135 cm	7.5 YR brown silt	2.1	17.2	56.9	23.8
R 16	Robertson Cave Pit 1 160 cm	7.5 YR brown silt	3.8	15.9	55.8	24.4
R 20	Pit 2 170 cm	7.5 YR yellowish brown sand	2.4	26.5	44.7	26.4
R 28	Pit 2 195 cm	2.5 YR pale yellow sand	6.6	64.5	27.9	1.0
R 30	Pit 2 220 cm	7.5 YR brown silt	2.9	13.1	43.2	40.8
R 32b	Pit 3 335 cm	7.5 YR yellowish brown sandy silt	1.3	24.7	40.6	33.4
R 32c	Pit3 340 cm	5 YR reddish brown silt	3.9	15.3	32.3	48.5
R 34	Pit 3 355 cm	7.5 YR brown sandy silt	1.4	24.4	59.3	15.0
R 61	Pit 3 460 cm	10 YR dark brown sandy silt	3.3	3.4	57.0	36.3
Wet Cave						
Wp1d	Wet Cave Pit 1 40 cm	10 YR dark brown silt	12.1	43.3	21.5	23.1
Wp1h	Pit 1 85 cm	7.5 YR brown sandy silt	1.6	27.6	65.9	4.9
W 2	Pit 2 170 cm	2.5 YR pale yellow sand	0.5	52.5	45.7	1.3
W 4	Pit 2 190 cm	5 YR yellowish red sand	2.9	33.6	56.3	7.2
W 8	Pit 2 210 cm	5 YR yellowish red silt sand	3.0	33.5	53.2	10.2
W 10	Pit 2 225 cm	5 YR reddish brown sandy silt	13.6	23.9	41.8	20.7

Table 1 (*continued*)

Sample	Location	Description	>C. Sand	M. Sand to F. Sand	V.F. Sand to C. Silt	<C. Silt
			mm (>0.5)	(0.5 to 0.3)	(0.3 to 0.1)	<0.1
Wet Cave						
W 15	Pit 2 335 cm	5 YR reddish brown sandy silt	4.3	26.2	45.3	24.3
Main Fossil Chamber; Victoria Cave						
VF1	Pit C 20 cm	7.5 YR yellowish brown sand	3.2	50.0	44.1	2.7
VF4	Pit C 40 cm	5 YR reddish silty sand	5.2	43.2	47.4	4.2
VF6	Pit B 80 cm	2.5 YR grey yellowish sand	2.9	46.2	50.0	1.6
Starburst Chamber; Victoria Cave						
SB1	Pit B 20 cm	5 YR reddish silt	17.3	45.7	31.3	9.0
SB2	Pit B 60 cm	5 YR reddish silt	29.3	44.1	23.0	5.0
Grant Hall; Victoria Cave						
GH1	Pit 1 10 cm	7.5 YR brown silty sand	36.7	34.9	21.7	6.7
Blanche Cave						
B2	Pit 1 38 cm	7.5 YR yellowish brown sand	4.8	17.3	34.6	43.3
B4	Pit 1 50 cm	7.5 YR brown sandy silt	5.5	20.3	38.2	35.9
B8	Pit 1 95 cm	5 YR reddish brown sandy silt	7.5	29.8	44.1	18.6

fine-grained material, having a considerable very fine sand to silt component.

Petrographical thin sections of several representative samples were examined in order to characterize the physical attributes of the cave sediments (Fig. 2). Apparently all three horizon types are comprised of varying amounts of quartz silt aggregates consisting of iron oxides and clays, weathered rock fragments (sedimentary and limestone), organic matter, and bone fragments. Deposit type I-a pale yellow (2.5YR) homogeneous sand—is almost entirely dominated by quartz grains (>80%) that display undulose extinction, have moderate sphericity, and are predominantly subrounded, of medium grain size (>0.5 cm), and moderately sorted. The remainder of the thin section is comprised of minor amounts of organic matter materials, sedimentary rock fragments, and clay mineral/iron oxide aggregates. Deposit type II-brown (7.5YR and 5YR) sandy silt horizons—contains 50% approximately quartz grains that display undulose extinction, have low sphericity, and are subangular, poorly sorted, and of medium to fine grain size (>0.5 cm). This reduction in quartz content in comparison to the yellow sands corresponds to an increase in the amount of organic matter and silt. Deposit type III consists of reddish (2.5 YR and 5 YR) sandy silts that are comprised of less quartz (40%). The quartz grains display undulose extinction, have low sphericity and generally are fine-grained (<0.5 cm), subrounded, and moderately sorted. A significant amount of reddish fine silt groundmass is also evident in the sample (50%) and appears to be an aggregate of iron oxides and clay minerals. The remaining 5–10% consists of organic matter and aggregates of soil particles.

4.2. Major and trace elemental geochemistry (XRF)

4.2.1. Major elemental geochemistry of cave sediments

Major elemental analysis was also undertaken on the same six cave deposits and many of the regional surficial deposits, with results presented in Table 2. The majority of the cave horizons exhibit a very high percentage of SiO_2, up to 95% in some cases, with SiO_2 being more prominent in the homogeneous sand horizons, reflecting their high quartz component. Al_2O_3 and Fe_2O_3 contents range between 2% and 15%, increasing in the silt horizons corresponding to a decrease in SiO_2 content (Fig. 3A). These increases are a reflection of clay and iron oxide content in the fine-grained fraction. Loss on ignition (LOI)–which is an indicator of the combined organic matter, hydrated, and carbonate mineral phase content within a sediment medium (e.g., Craft et al., 1991)–is also significant in many cave horizons. LOI also increases relative to decreasing SiO_2 content (Fig. 3B) and is most prevalent in the organic matter and silt-rich horizons of the younger deposits (Fig. 3C), especially Robertson Cave (up to 15%). Total base cation content (Na_2O, K_2O, CaO, and MgO) is low (<5% in total) in all caves, with the exception of CaO, which is a significant component in horizons where SO_3 is high. Those horizons with high CaO and SO_3 have been identified by Forbes and Bestland (in press) and Forbes et al. (in press) as sediments dominated by accumulations of guano and weathered fragments of cave limestone, thus reflecting processes occurring within the cave.

4.2.2. Major elemental geochemistry (XRF) of surficial deposits

Comparisons of major elemental composition between the cave sediments and the surficial deposits of the

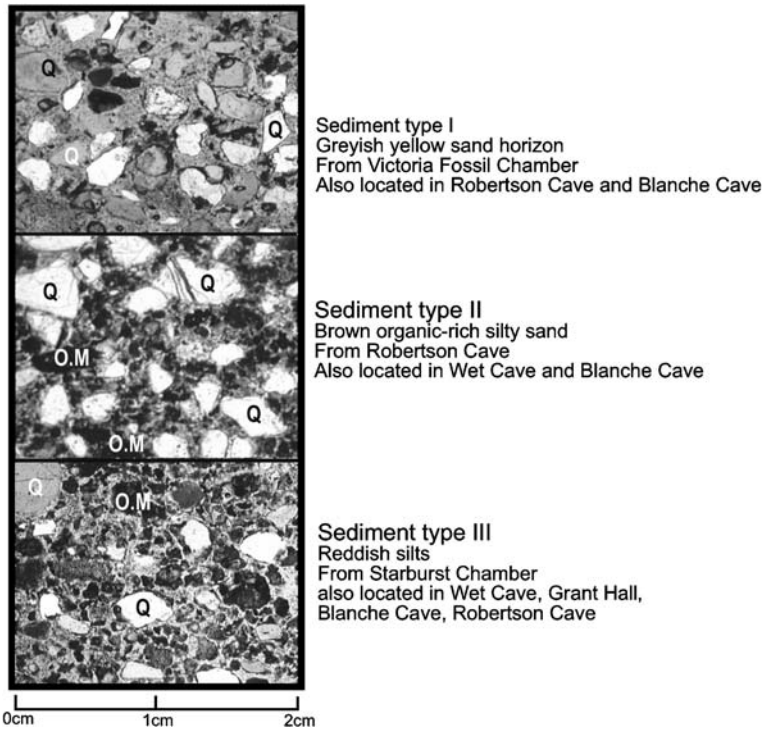

Fig. 2. Thin section petrography for three main types of cave deposits. Q refers to quartz and O.M. to organic matter.

Naracoorte region are presented in Fig. 4 and Table 2. The Bool Lagoon lunettes have significantly less SiO_2 content (60%) and higher Al_2O_3 (15%), MgO (2%), Fe_2O_3 (5–6%), and LOI (9–12%) than the cave sediments. The Coonawarra RBE's A and B horizons also exhibit lower SiO_2 contents in comparison to the cave sediments. Although the A horizons contain more SiO_2 and less Al_2O_3, Fe_2O_3, and LOI, reflecting the higher sand/quartz content, compared to the clay-rich B Horizons, which have larger Al_2O_3 and Fe_2O_3 contents.

The surficial sand and relict dune units of the upper SE (Bridgewater Formation, the fine podsolic sand unit near Robertson Cave, and the modern sand at Robe) are all dominated by SiO_2 (in excess of 95%). Sediments from the Lower Murray and Coorong regions also contain varying but substantial amounts of SiO_2, reflecting their various quartz sand contents. Sandy sediments from Woods Well (located midway down the Coorong) consist predominantly of SiO_2 (95%); in comparison, more silt-dominated floodplain sediments at both Meningie and Kingston have SiO_2 contents below 80%. This decrease in SiO_2 is compensated for by increases in Al_2O_3 (5%), Fe_2O_3 (<2%), and LOI (13%). Sand deposits from the banks of the Lower Murray at Wellington are 90% SiO_2, with the overbank sediment on the eastern side of the river containing minor amounts of Al_2O_3 (4%).

4.2.3. Trace elemental geochemistry (XRF) of cave and surficial deposits

Trace elemental data presented in Table 3 and illustrated in Fig. 4 identify relationships between the cave sediments and many of the regional surficial deposits. Trace elements such as V, Ba, Co, Ni, Pb, and Sc appear similar in concentrations for the cave sediments and many of the sand-dominated surficial deposits such as the Coorong and Lower Murray sands, RBE sandy A horizons, and podsolic sands. The more silt-dominated surficial deposits, like the RBE's B horizons and lunettes, have higher contents of most of these trace elements in comparison to the cave sediments.

These trends are even more apparent when investigating the elements Ti, Zr, Ce, and Ti. Comparisons of Ti/Zr ratios and TiO_2 concentrations for cave deposits and the regional surficial deposits (Fig. 5A) see the entire suite of cave deposits falling between the finer grained deposits (such as the lunettes and RBE B horizons) and the coarser regional sand units. Comparisons of the concentrations of the trace elements Y and Ce (Fig. 5B) see a similar trend emerge with the cave sediments. However, the cave sediments appear more akin to the sand-rich deposits rather than the silt-rich deposits. Ti, Zr, Ce, and Y data obtained for other regional deposits [like metamorphic units from the Adelaide geosyncline (Turner et al., 1993)

Table 2
Major and trace elemental (XRF) data for cave sediments and regional surficial deposits

#	SiO_2	Al_2O_3	Fe_2O_3	MnO	MgO	CaO	Na_2O	K_2O	TiO_2	P_2O_5	SO_3	LOI	Total	Zr	Y	Ce
Naracoorte Cave sediments																
R 0	70.7	8.1	4.5	0.0	0.2	0.1	0.1	0.5	0.5	0.3	0.0	14.2	99	173	11	30
R6	88.8	3.6	1.3	0.0	0.1	0.4	0.1	0.2	0.3	0.2	0.0	3.8	99	147	5	9
R 12	88.9	4.0	1.0	0.0	0.1	0.1	0.1	0.3	0.3	0.1	0.0	4.4	99	185	7	17
R 16	84.6	5.4	2.6	0.0	0.1	0.1	0.1	0.4	0.4	0.1	0.0	5.7	100	163	8	18
R 20	85.3	4.8	1.7	0.0	0.2	0.5	0.1	0.5	0.4	0.4	0.0	5.4	99	205	15	29
R 28	91.3	3.2	1.1	0.0	0.1	0.2	0.1	0.3	0.3	0.1	0.0	2.9	99	99	5	13
R 30	79.8	5.9	2.3	0.0	0.3	1.6	0.2	0.6	0.5	0.8	0.0	7.1	99	206	17	41
R 32b	94.3	1.6	0.5	0.0	0.0	0.2	0.1	0.2	0.2	0.1	0.0	2.9	100	92	5	9
R 32c	38.5	1.4	2.9	0.0	0.4	16.5	0.3	0.3	0.2	2.3	18.9	19.6	101	75	8	22
R 36	97.6	0.5	0.2	0.0	0.0	0.0	0.0	0.1	0.1	0.0	0.0	1.1	100	83	3	5
R 61	77.0	5.7	2.6	0.0	0.3	2.9	0.2	0.6	0.4	1.5	0.4	8.1	100	174	18	36
Wp1d	63.7	2.1	0.8	0.0	0.4	11.9	0.1	0.2	0.2	0.1	15.7	5.8	101	96	5	6
Wp1h	95.3	1.7	0.7	0.0	0.0	0.0	0.0	0.3	0.2	0.0	0.0	1.2	100	112	4	10
W 2	96.8	1.2	0.2	0.0	0.1	0.0	0.0	0.2	0.2	0.0	0.0	0.7	99	72	3	2
W 4	91.3	2.8	1.1	0.0	0.1	0.2	0.1	0.3	0.2	0.1	0.0	2.1	98	114	7	20
W 8	93.1	2.9	1.2	0.0	0.0	0.0	0.1	0.3	0.3	0.0	0.0	1.7	100	114	7	20
W 10	86.1	6.6	2.5	0.0	0.1	0.1	0.1	0.5	0.4	0.1	0.0	3.4	100	107	5	9
W 15	90.8	2.6	1.3	0.0	0.2	1.4	0.1	0.3	0.2	0.8	0.0	1.8	99	158	9	20
SB1	88.3	4.6	1.8	0.0	0.2	0.1	0.0	0.2	0.3	0.0	0.0	2.1	98	135	6	14
SB2	81.4	9.0	4.3	0.0	0.4	0.1	0.1	0.4	0.4	0.0	0.0	4.1	100	143	18	46
VF1	91.3	3.8	2.0	0.0	0.2	0.1	0.1	0.3	0.3	0.1	0.0	1.8	100	238	9	20
VF4	94.2	2.9	0.7	0.0	0.1	0.0	0.0	0.2	0.2	0.0	0.0	1.5	100	118	4	11
VF6	98.4	0.7	0.2	0.0	0.0	0.0	0.0	0.1	0.2	0.0	0.0	0.4	100	158	3	11
B2	80.0	6.3	2.9	0.0	1.1	2.1	0.5	0.8	0.4	0.2	0.1	8.0	102	163	21	50
B3	96.0	1.4	0.6	0.0	0.0	0.1	0.1	0.3	0.1	0.0	0.0	0.9	100	64	4	5
B4	85.4	4.9	2.2	0.0	0.2	0.1	0.2	0.7	0.4	0.0	0.0	5.6	100	174	8	19
B5	66.0	12.7	6.5	0.0	0.9	0.2	0.4	1.5	0.9	0.2	0.0	10.2	99	216	31	82
B6	82.3	7.3	3.6	0.0	0.5	0.2	0.2	1.0	0.5	0.1	0.0	4.3	100	173	14	38
B7	83.1	5.6	2.8	0.0	0.3	0.1	0.2	0.8	0.5	0.1	0.0	6.2	100	174	13	34
B8	90.4	4.1	2.1	0.0	0.3	0.1	0.2	0.6	0.3	0.1	0.0	2.4	100	118	7	16
B9	65.5	5.1	2.7	0.0	0.3	9.0	0.2	0.5	0.3	0.2	9.6	7.4	101	119	7	20
GH1	71.8	12.9	6.4	0.0	0.5	0.1	0.1	0.5	0.5	0.2	0.0	6.9	100	127	5	8
Surficial deposits of the Naracoorte Region																
BL1	62.2	15.7	6.0	0.0	2.2	0.7	0.2	2.3	0.8	0.0	0.0	9.9	100	138	9	20
BL2	62.7	15.7	6.0	0.0	2.3	0.6	0.2	2.4	0.8	0.0	0.0	9.2	100	177	12	27
BL4	60.3	14.5	5.7	0.0	2.0	0.9	0.2	2.3	0.8	0.0	0.0	12.7	99	209	14	31
ML	62.6	14.0	5.3	0.0	2.4	2.0	0.3	2.0	0.8	0.0	0.0	10.9	100	173	11	20
BW	97.6	0.6	0.8	0.0	0.1	0.0	0.0	0.3	0.0	0.0	0.0	0.3	100	26	1	5
RSQN	99.3	0.3	0.1	0.0	0.0	0.0	0.0	0.1	0.1	0.0	0.0	0.8	101	102	2	5
RSQS	88.1	5.4	1.7	0.0	0.2	0.0	0.1	0.4	0.4	0.1	0.0	3.3	100	128	7	17
RS	96.1	1.4	0.7	0.0	0.0	0.1	0.2	0.5	0.1	0.0	0.0	0.7	100	59	4	7
11SB	83.0	7.0	3.2	0.0	0.4	0.2	0.5	1.2	0.4	0.0	0.0	4.1	100	141	11	24
TRRP	64.3	16.9	7.2	0.0	0.5	0.1	0.1	0.5	0.6	0.0	0.0	8.8	99	171	12	30
MMG	72.9	13.0	1.7	0.0	0.3	0.5	3.3	5.5	0.2	0.0	0.0	0.5	98	237	39	121
RRG	71.8	12.0	2.7	0.0	0.5	1.3	3.2	4.4	0.4	0.0	0.0	0.3	97	271	52	102
Surficial deposits of the Lower Murray and Coorong																
MFP	78.5	4.3	1.3	0.0	0.4	0.3	0.3	1.0	0.3	0.1	0.0	13.2	100	138	7	20
CWW	94.6	1.6	0.3	0.0	0.1	0.1	0.2	0.6	0.2	0.0	0.0	0.8	98	264	5	10
KFM	77.1	5.0	1.3	0.0	0.4	0.2	0.4	1.1	0.4	0.1	0.0	13.2	99	113	8	16
WM2	86.0	4.3	1.0	0.0	0.2	0.1	0.4	1.1	0.3	0.0	0.0	1.9	95	182	9	19
WMW	96.0	1.7	0.2	0.0	0.1	0.1	0.3	0.5	0.1	0.0	0.0	0.8	100	115	6	10

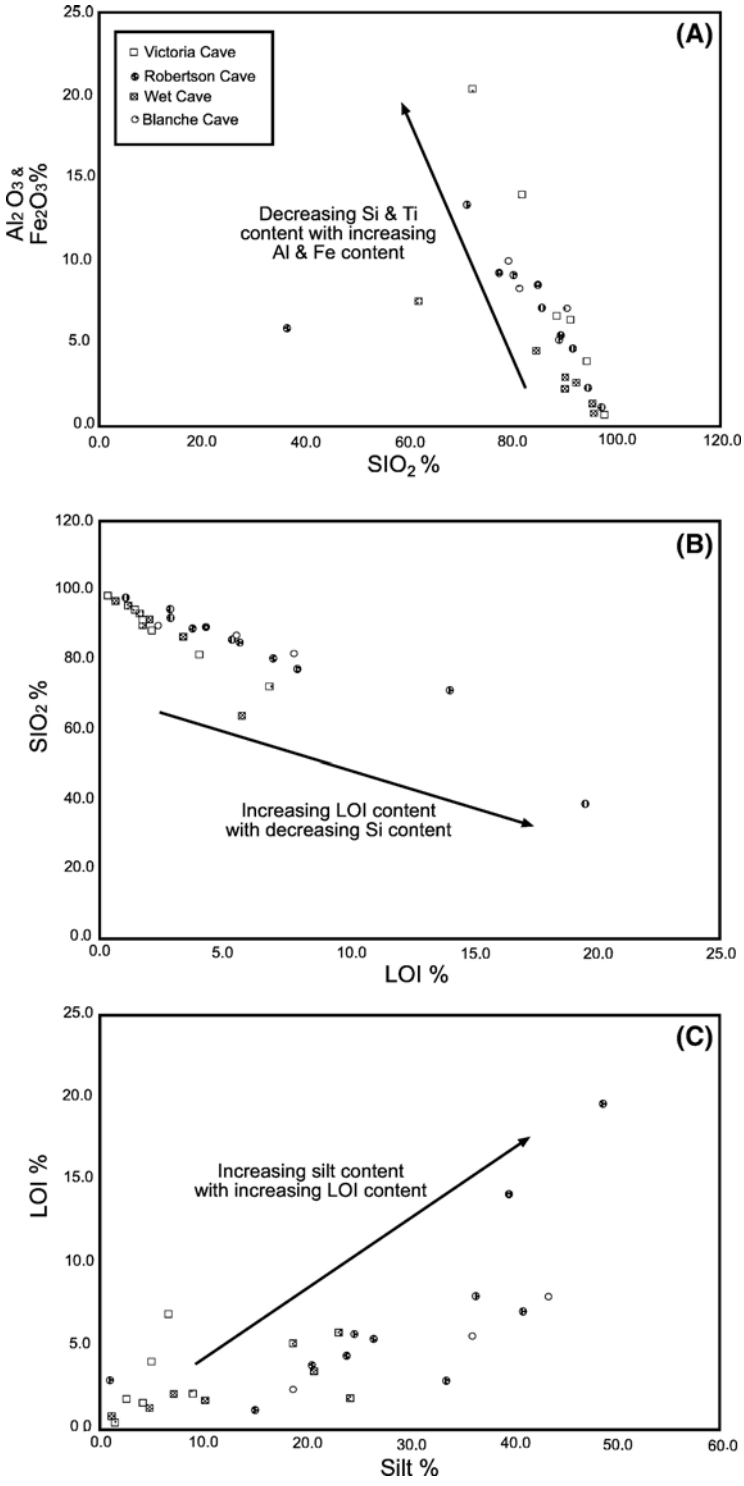

Fig. 3. (A) SiO_2 vs. Al_2O_3 and Fe_2O_3. (B) LOI vs. SiO_2. (C) LOI vs. silt contents for cave deposits.

and Murray River silts (Douglas et al., 1995, 1999)] allow for an appreciation of the relationship between these deposits and the cave sediments. The metamorphics are similar in trace element composition to the silt RBE's B horizons and lunettes, while the Murray River silts are more similar to the cave deposits.

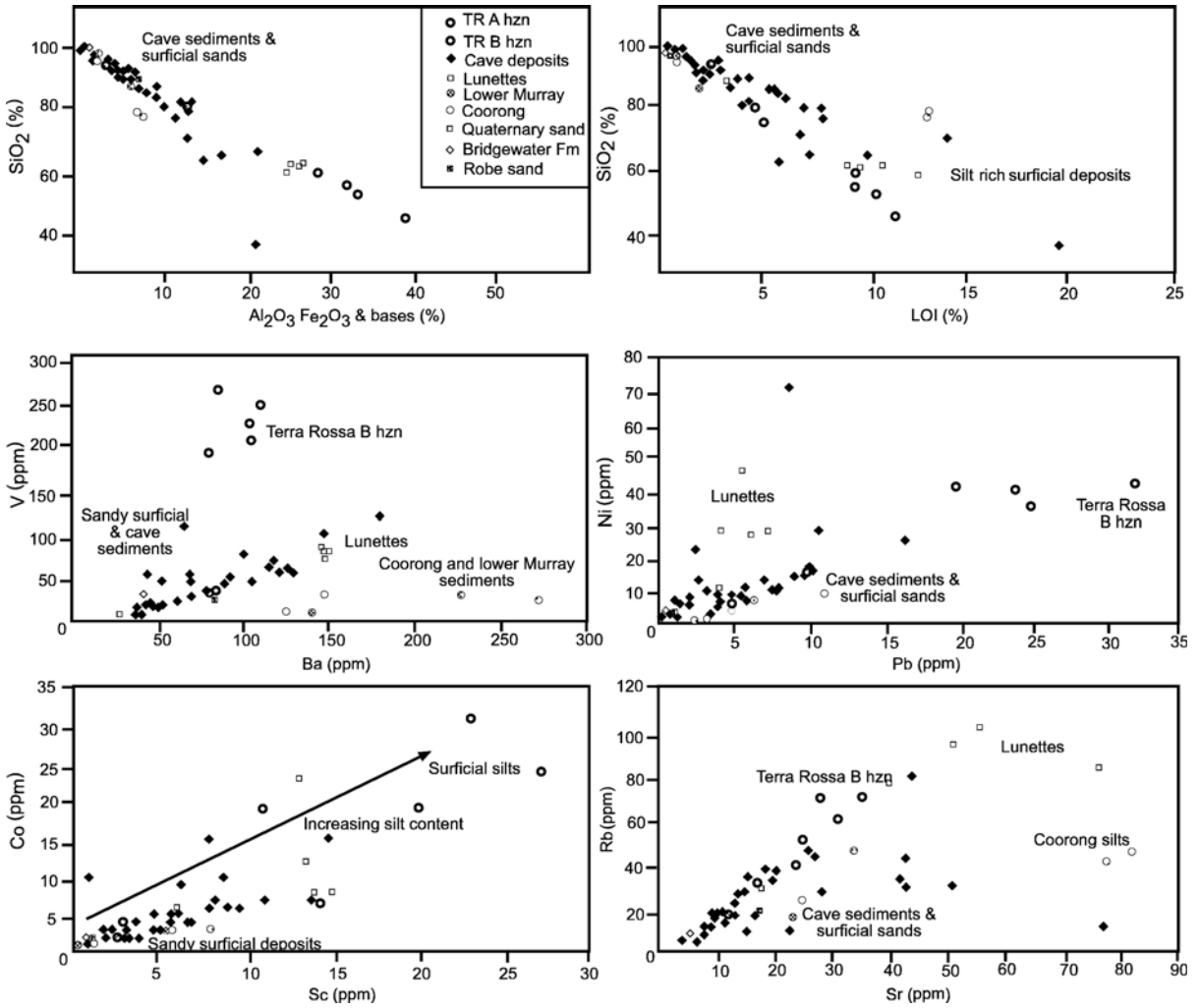

Fig. 4. Comparisons of major and trace elemental data between cave sediments and regional surficial deposits.

4.3. Sediment mineralogy (XRD)

4.3.1. Cave sediment mineralogy

The mineral component of several cave sediment horizons were quantified via XRD analysis and are presented in Fig. 6. Identified is a dominance by various amounts of quartz, clay minerals, and iron oxides. The mineral content of the homogeneous yellow sand horizons of Robertson and Wet Caves are, as expected, mostly quartz (70–90%), with little representation from any other minerals. Similar sandy horizons located in Blanche Cave are dominated by quartz, but also have contributions from calcite (<15%). In comparison to the sand-dominated units, the reddish silt horizons and the brownish organic matter rich horizons have significantly higher percentages of clay minerals (kaolinite and smectite) and iron oxides, with a corresponding reduction in quartz. This change is more evident in the reddish silts rather than the brownish sandy silts where clay mineral content represents up to 60%. An exception to the quartz and clay mineral dominance is the presence of phosphate minerals (whitlockite and apatite) in a red silt layer toward the base of the Robertson Cave deposit. These minerals have been shown to be the product of in situ reactions between fine-grained clastic material (silts and limestone) and decomposed bat guano (e.g., Forbes and Bestland, in press; Forbes et al., in press).

4.3.2. Mineralogy of surficial deposits

Mineralogical composition of the surficial deposits of the greater SE of South Australia are presented in Fig. 7, including the RBE soil profiles at Padthaway and Coonawarra, which have had extensive mineralogical

Table 3
Trace elemental (XRF) data for cave sediments and regional surficial deposits

#	Zr	Y	Ce	Rb	Pb	Ni	Ba	Sc	Co	V
Naracoorte Cave sediments										
R 0	173	11	30	37	10	16	147	11	7	97
R6	147	5	9	16	1	7	50	4	2	23
R 12	185	7	17	22	4	7	70	5	3	27
R 16	163	8	18	26	4	9	69	7	4	52
R 20	205	15	29	27	8	10	89	6	5	42
R 28	99	5	13	13	2	6	50	3	2	22
R 30	206	17	41	32	7	13	115	9	6	60
R 32b	92	5	9	9	3	13	38	1	10	13
R 32c	75	8	22	12	9	14	78	6	4	35
R 36	83	3	5	4	0	6	40	1	1	8
R 61	174	18	36	30	8	11	121	7	4	55
Wp1d	96	5	6	9	2	8	43	6	9	18
Wp1h	112	4	10	11	4	3	52	2	3	17
W 2	72	3	2	8	1	3	39	1	1	8
W 8	114	7	20	17	4	5	69	2	3	45
W10	107	5	9	16	3	4	62	3	2	22
W 15	158	9	20	32	6	11	100	10	6	75
SB1	135	6	14	18	3	10	44	7	4	52
SB2	143	18	46	34	11	28	65	14	7	106
VF1	238	9	20	18	6	7	52	5	3	45
VF4	118	4	11	17	1	6	46	3	3	19
VF6	158	3	11	5	1	2	37	1	2	8
GH1	127	5	8	17	2	6	47	4	4	17
B2	163	21	50	42	10	15	129	8	7	55
B4	174	8	19	37	6	8	105	6	5	44
B8	118	7	16	28	5	9	78	5	5	39
Surficial deposits of the Naracoorte Region										
BL1	138	9	20	76	4	28	147	15	8	80
BL2	177	12	27	94	6	27	149	14	8	79
BL4	209	14	31	101	7	28	146	14	12	82
ML	173	11	20	83	6	46	148	13	23	70
BW	26	1	5	9	1	4	42	1	2	30
RSQN	102	2	5	3	0	5	28	1	1	7
RSQS	128	7	17	29	4	11	80	6	6	41
RS	59	4	7	19	1	3	83	1	2	24
11SB	141	11	24	57	11	17	198	6	11	71
TRRP	171	12	30	48	14	43	56	13	33	125
MMG	237	39	121	194	13	1	346	4	2	7
RRG	271	52	102	218	21	3	604	5	5	25
Surficial deposits of the Lower Murray and Coorong										
MFP	138	7	20	41	11	9	272	6	3	24
CWW	264	5	10	23	3	2	125	1	1	10
KFM	113	8	16	45	5	5	148	8	3	30
WM2	182	9	19	46	6	7	227	6	3	28
WMW	115	6	10	15	2	1	140	0	1	7

analysis undertaken on them (Green et al., 2004; Mee et al., 2004). The composition of the RBE's sandy A horizons appear to be almost entirely quartz (90%), while the B horizons are predominantly clay minerals (>60%) and iron oxides (10–15%). Variation in the clay mineral type is apparent between the two localities, with kaolinite and illite predominating at Padthaway, while around Coonawarra (and also Naracoorte) smectite and kaolinite dominate. The mineralogical content of the fine silt lunettes deposited at Bool Lagoon consists of the clay minerals illite (15–30%) and smectite (15–20%) and minimal amounts of kaolinite (2%), as well as calcite (50%) and quartz (10%).

The surficial sand units of the upper SE have mineral compositions that are dominated by quartz and carbonates. The modern dune system at Robe consists of aragonite (54%), magnesium-calcite (18%), and calcite (22%), plus a minor amount of quartz (6%). In comparison, the Pleistocene-aged Bridgewater Formation is mainly calcite (70%) and quartz (22%) with some small contributions from goethite (6%) and orthoclase (1%). The limestone and calcareous sandstones that underlie the RBEs of the Coonawarra and Naracoorte area are also of similar mineralogical content (Mee et al., 2004). For example, the underlying calcareous sandstone exposed in the Gartners Quarry at Coonawarra was found to be over 90% calcite, with the residuum post-$CaCO_3$ removal consisting of over 90% quartz. The Gambier limestone exposed at the Joanna profile indicated a 95% calcite and 5% quartz composition, with its post-$CaCO_3$ removed residuum consisting of quartz (65%) and smectite (35%).

The mineralogy of the silty sands and sands of the lower reaches of the Murray River at Wellington consists almost entirely of quartz (96%) with only minor amounts of albite (3%) and orthoclase (1%). The sandy silt located on the Coorong floodplain at Kingston consists of a variety of minerals including the carbonates Mg-calcite (46%) and aragonite (19%), quartz (10%), smectite (14%), and ankerite (14%). By comparison, the sandy Coorong unit at Woods Well is dominated by quartz (70%) and aragonite (19%). Also evident are minor amounts of calcite (6%), albite (1–2%), and halite (2%).

The granitic outcrop at Mt. Monster consists of the feldspar minerals orthoclase (40%) and albite (40%), chlorite (19%), and quartz (10%), with a minor contribution of illite (3%). A reddish, poorly developed soil that formed on a basalt deposit associated with the extinct volcano Mt. Watch near Millicent, has a mineral composition that consists predominantly of pyroxene (augite) (37%) and the clay minerals smectitie (18%), illite (15%), and halloysite (12%). Also identified are minor amounts of hematite (4%), quartz (1%), forsterite (6%), and analcime (6%). The presence of the mineral halloysite is indicative of soils of basaltic origins (Hosking et al., 1957), as are augite (pyroxene) and forsterite (olivine).

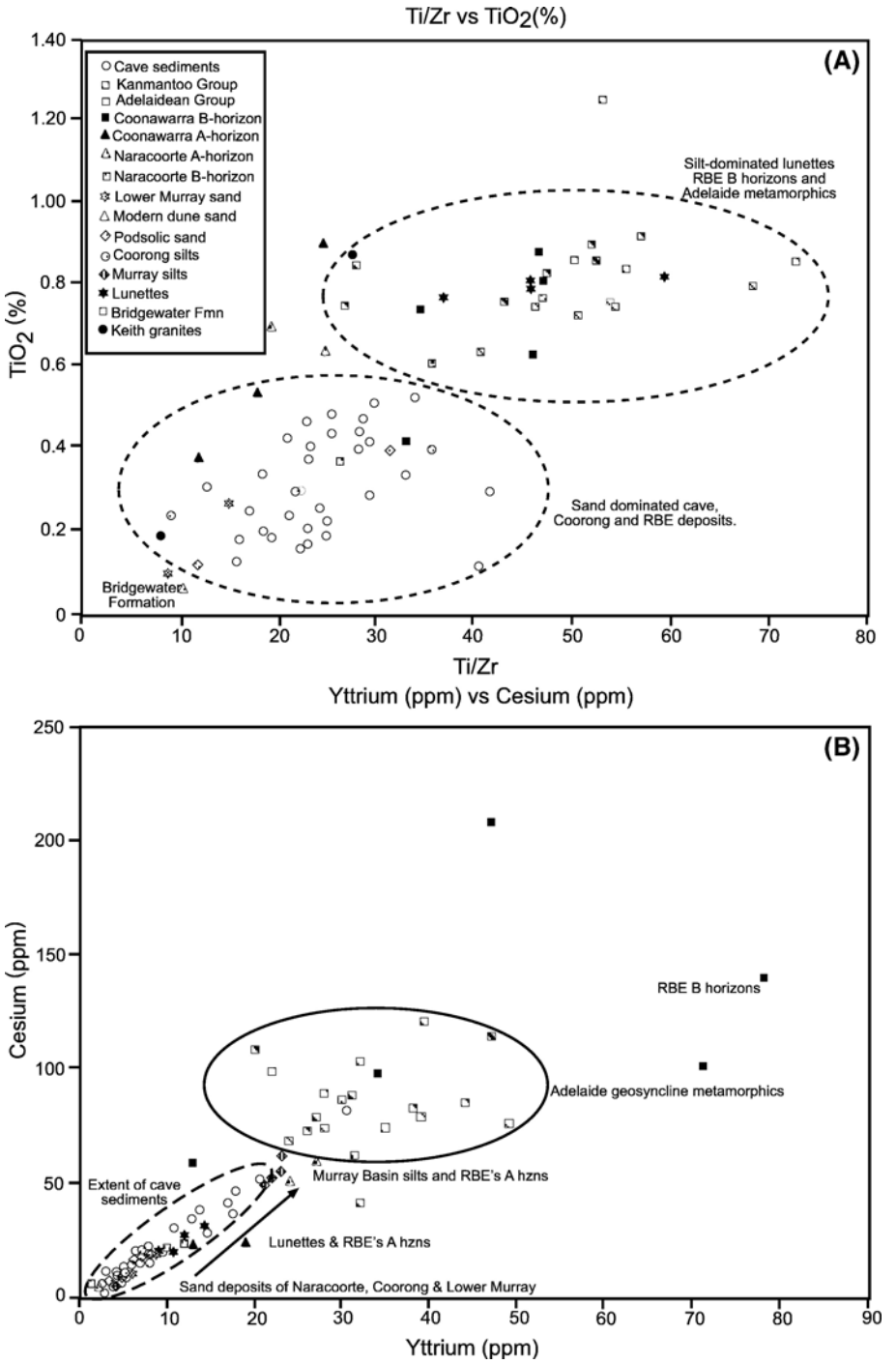

Fig. 5. (A). Zr/Ti vs. Ti concentrations. (B). Ce vs. Y for cave and surficial deposits of the Naracoorte region and silts from the Murray River.

4.4. Strontium isotope geochemistry

4.4.1. $^{87}Sr/^{86}Sr$ ratios and Sr concentrations for the Naracoorte Cave sediments

The strontium isotopic ratios ($^{87}Sr/^{86}Sr$) and concentrations (ppm) for the Naracoorte Cave sediments and surficial deposits of the SE region are presented in Table 4. $^{87}Sr/^{86}Sr$ ratios were determined for 26 various sedimentary horizons from the six cave chambers, with all falling within the narrow range of 0.710 and 0.725 (avg 0.723; $n=27$). The removal of three outliers (SB2, GH1, and B2), which are all significantly lower, further

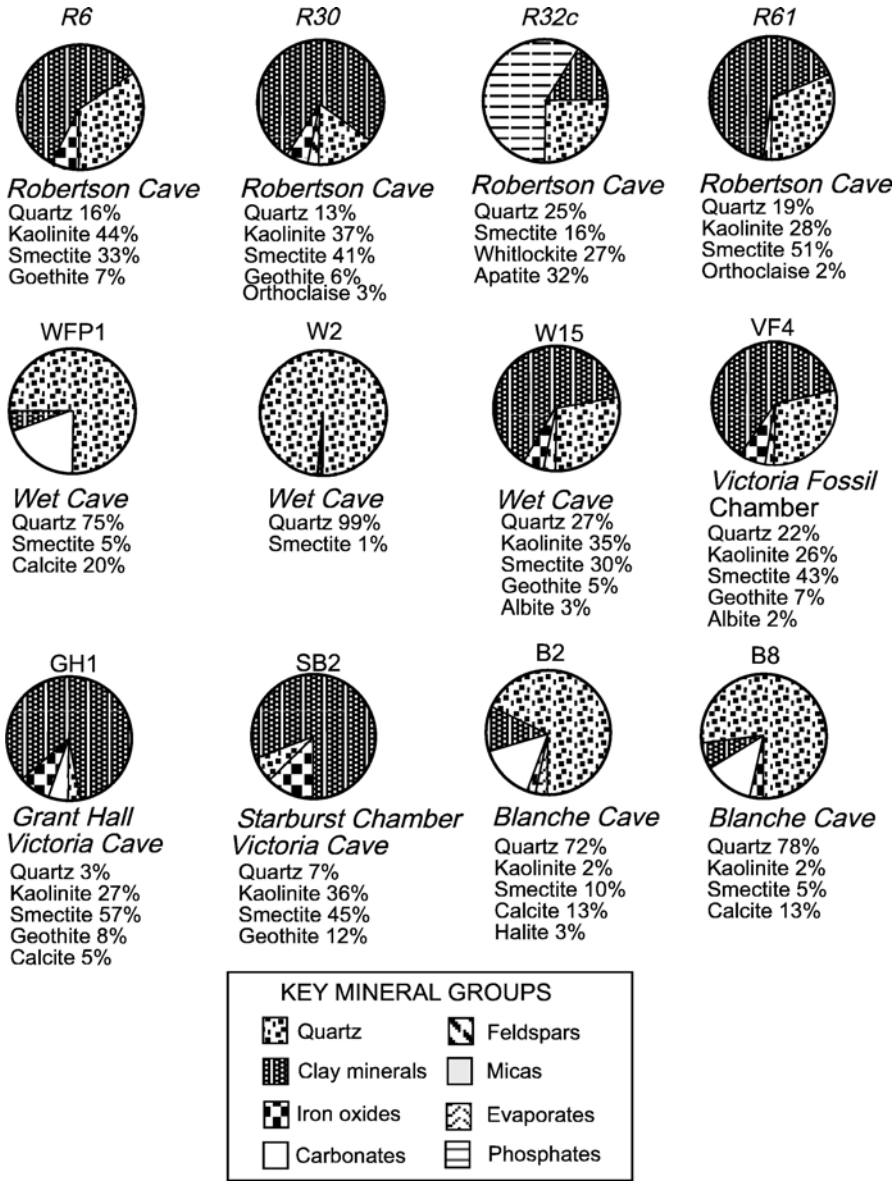

Fig. 6. Mineralogical composition of the Naracoorte Cave sediments.

reduces the range of the data set to 0.720–0.725. The lower values obtained for these sediment horizons are more than likely a result of the carbonate fraction not being completely removed prior to analysis. Average $^{87}Sr/^{86}Sr$ ratios for each of the six cave deposits also see a close correlation: Robertson Cave 0.724 ($n=11$), Wet Cave 0.724 ($n=6$), Blanche Cave 0.724 ($n=3$), and Victoria Cave 0.721 [including Starburst Chamber 0.720 ($n=2$), Grant Hall 0.720 ($n=1$), and Main Fossil Chamber 0.723 ($n=3$)], all of which are accurate to two significant figures.

In comparison to the $^{87}Sr/^{86}Sr$ ratios, the strontium concentrations vary widely, ranging between 3 and 80 ppm, although most horizons have concentrations 30 ppm or lower. Plots of $^{87}Sr/^{86}Sr$ ratios and strontium concentrations (Fig. 8A) identify a lack of any significant relationship between the isotopic ratio and the strontium concentration. Yet strontium concentrations in the cave sediments appear to increase corresponding to increasing silt content ($R^2=0.597$), with concentrations at their lowest in the yellowish sand horizons and their highest in some of the brownish and reddish sandy silts

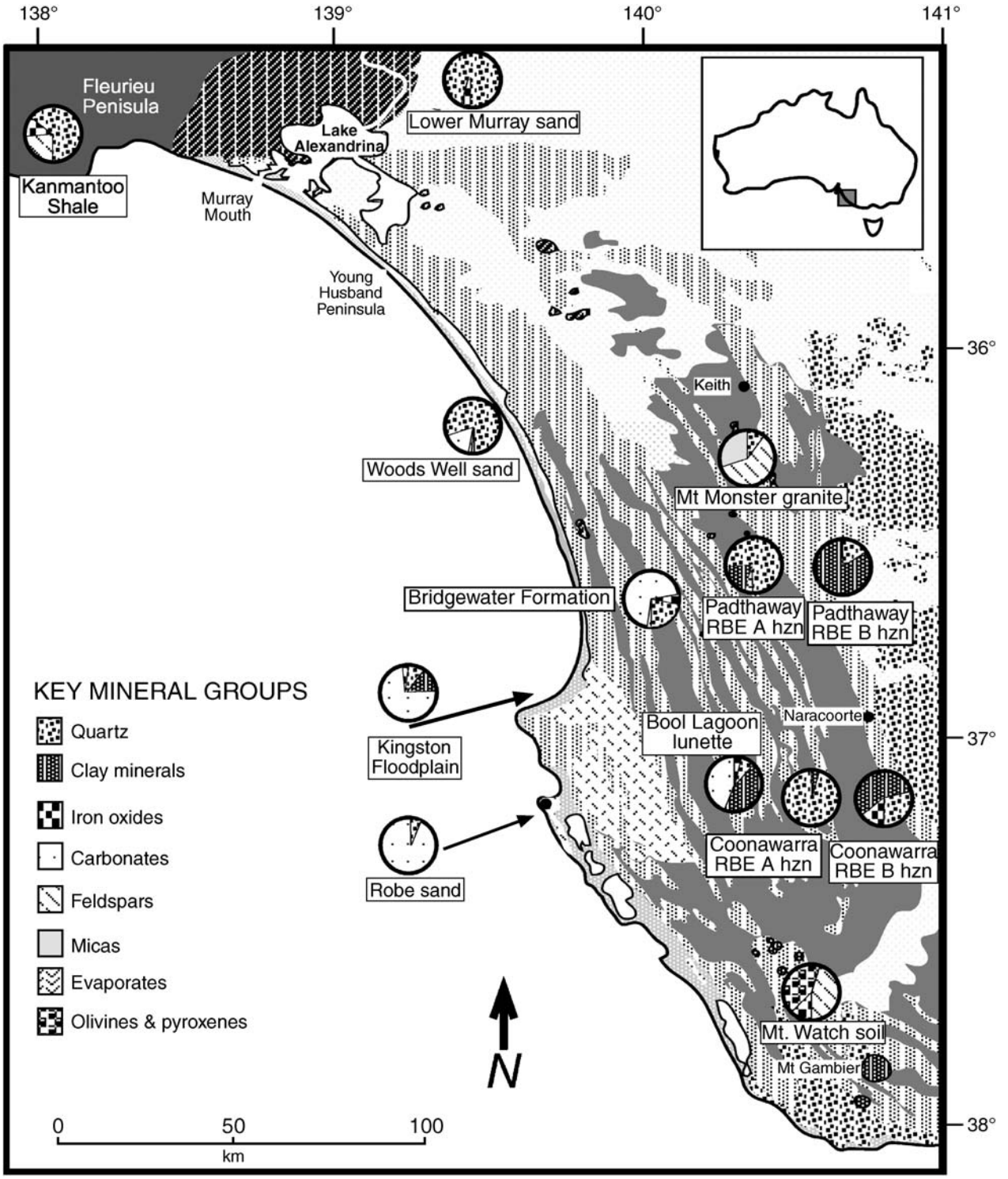

Fig. 7. Map of SE South Australia displaying the mineralogical composition of major surficial units.

Table 4
$^{87}Sr/^{86}Sr$ ratios and strontium concentrations for both cave deposits and regional surficial units

Sample	Location	Sr (ppm)	$^{87}Sr/^{86}Sr$[a]	S.D.[b]
Cave deposits				
R 0	Robertson Cave	18	0.7226	0.00005
R 6	Robertson Cave	9	0.7228	0.00005
R 12	Robertson Cave	13	0.7232	0.00007
R 16	Robertson Cave	14	0.7246	0.00008
R 20	Robertson Cave	28	0.7240	0.00006
R 28	Robertson Cave	11	0.7244	0.00006
R 30	Robertson Cave	42	0.7255	0.00006
R 32b	Robertson Cave	15	0.7226	0.00020
R 32c	Robertson Cave	77	0.7230	0.00005
R 34	Robertson Cave	7	0.7238	0.00006
R 61	Robertson Cave	51	0.7234	0.00006
Wp1h	Wet Cave	9	0.7240	*
W 2	Wet Cave	8	0.7222	0.00041
W 4	Wet Cave	17	0.7253	0.00007
W 8	Wet Cave	13	0.7241	0.00005
W10	Wet Cave	20	0.7238	0.00007
W 15	Wet Cave	31	0.7238	0.00006
SB1	Starburst Chamber	10	0.7203	0.00006
SB2	Starburst Chamber	15	0.7188	0.00005
VF1	Victoria Fossil Chamber	11	0.7233	*
VF4	Victoria Fossil Chamber	9	0.7230	*
VF6	Victoria Fossil Chamber	4	0.7234	*
B2	Blanche Cave	42	0.7171	0.00006
B4	Blanche Cave	37	0.7280	0.00006
B8	Blanche Cave	28	0.7268	0.00006
GH1	Grant Hall	9	0.7198	0.00012
Surficial deposits of SE region				
BL1	Bool Lagoon lunettes	40	0.7255	0.00010
BL2	Bool Lagoon lunettes	51	0.7257	0.00006
BL4	Bool Lagoon lunettes	56	0.7144	0.00006
ML	Bool Lagoon lunettes	77	0.7239	0.00007
RS	Robe sand	17	0.7250	0.00007
BW	Bridgewater Formation	5	0.7443	0.00014
11SB	Harpers Ridge RBE	50	0.7209	0.00028
RSQS	Robertson Cave podsolic sand	18	0.7226	0.00005
TRRP	Robertson Cave entrance RBE	22	0.7167	0.00007
MMG	Mount Monster granite	46	0.7839	0.00016
Surficial deposits of the Lower Murray and Coorong region				
MFP	Meningie floodplain Coorong	78	0.7174	0.00006
CWW	Woods Wells Coorong	25	0.7244	0.00008
WM2	Wellington silty sand (east)	34	0.7301	0.00007
WMW	Wellington silty sand (west)	23	0.7277	0.00009
KFM	Kingston floodplain	82	0.7190	0.0006
Kangaroo Island				
RRG	Remarkable Rocks granite (KI)	74	0.7238	*

[a] Final results were normalised to the expected standard using replicate measurements of the standards NBS SRM 987-189 to 193.
[b] Standard deviations are on 100 replicate measurements of the sample.

(Fig. 8B). However, comparisons of $^{87}Sr/^{86}Sr$ ratios with silt content (Fig. 8C) show a distinct lack of correlation ($R^2=0.0021$).

4.4.2. $^{87}Sr/^{86}Sr$ ratios for the surficial deposits of the upper SE

$^{87}Sr/^{86}Sr$ and strontium concentrations for many of the surficial deposits of the greater SE region are compared to the cave deposits in Fig. 9. RBEs located in the Coonawarra (Green et al., 2004; Mee et al., 2004) and Padthaway (Green et al., 2004) areas (including the underlying calcareous bedrock) and the lunettes of Bool Lagoon have had their $^{87}Sr/^{86}Sr$ ratios examined in previous studies. $^{87}Sr/^{86}Sr$ ratios for many of these sedimentary deposits compare favourably with those determined for the cave sediments. The lunette silts (0.722; $n=4$) and the Coonawarra RBE's sandy A horizons (0.727; $n=5$), both surficial deposits proximal to the caves, provide the best correlation; while $^{87}Sr/^{86}Sr$ ratios for the clay-rich Coonawarra RBE's B horizons (0.718; $n=13$), Padthaway RBE's sandy A horizons (0.717; $n=3$), Naracoorte calcarenite (0.727, $n=1$), and clay B horizons (0.715; $n=6$) are all slightly lower than the $^{87}Sr/^{86}Sr$ ratios evident for the majority of the cave sediments.

$^{87}Sr/^{86}Sr$ ratios for the surficial sand units of the upper SE appear much more varied. The post-acid-treated residual (sand and silt) of the Pleistocene-aged, shell-laden Bridgewater Formation (0.744) is noticeably higher than the cave sediments. Another residual silt extracted from the calcareous sandstone at the base of the Gartners Quarry profile, which is thought to be part of the Bridgewater Formation, is also significantly higher (0.782; $n=2$) than the cave deposits. The homogeneous podsolic fine-sand deposit located near the entrance to Robertson Cave is almost identical to the $^{87}Sr/^{86}Sr$ ratios (0.724) observed for many of the cave sediments directly below; while the modern calcareous beach sand deposit located at Robe provided a similar ratio (0.725), which is also comparable to the results evident for the cave sediments.

$^{87}Sr/^{86}Sr$ ratios for sediments from the lower reaches of the Murray River and the Coorong are similar to those evident for the cave sediments and the surficial deposits of the Naracoorte region. Sandy river bank deposits located at Wellington reveal $^{87}Sr/^{86}Sr$ ratios of 0.730 (west bank) and 0.723 (east bank). At the northern end of the Coorong near Meningie, a $^{87}Sr/^{86}Sr$ of 0.714 was obtained for sandy silts; at Woods Well, where sediments are more sand-rich a $^{87}Sr/^{86}Sr$ ratio of 0.724 was obtained; while at Kingston at the Coorong's southern end, a lower ratio of 0.719 was evident for the sandy silts located there.

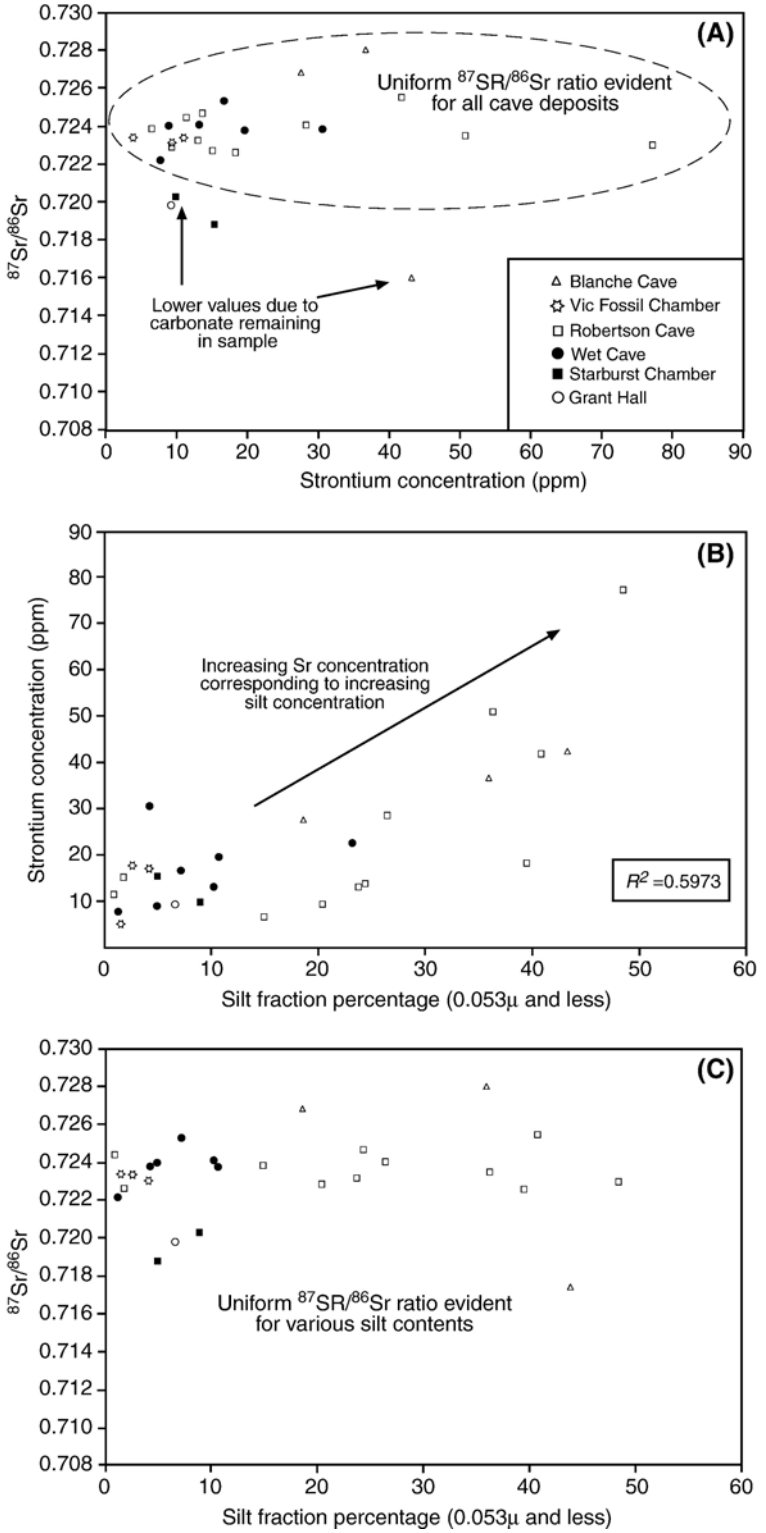

Fig. 8. Strontium isotope analysis for cave deposits. (A) $^{87}Sr/^{86}Sr$ vs. Sr concentration for various cave deposits. (B) Sr concentration vs. silt percentages for cave deposits. (C) $^{87}Sr/^{86}Sr$ vs. silt for cave deposits.

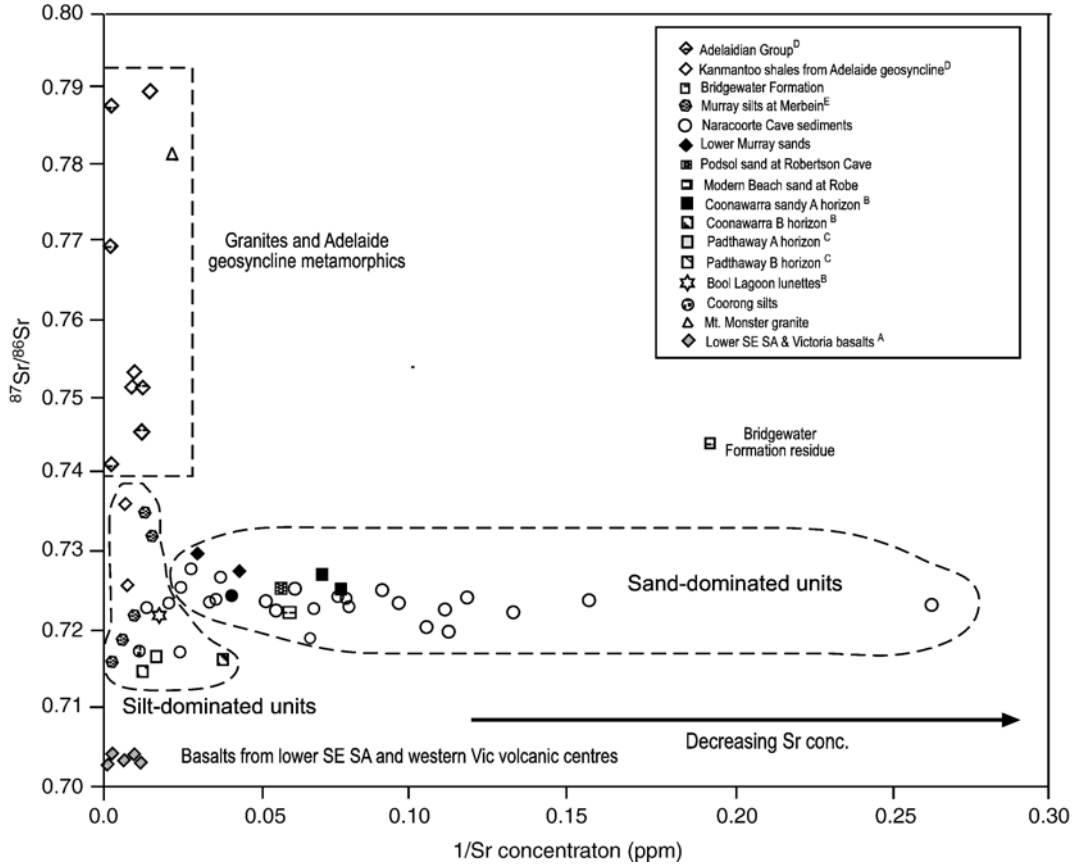

Fig. 9. $^{87}Sr/^{86}Sr$ vs. Sr for cave sediments and surficial sediments. Data presented from other studies includes; [A]Price et al., 1997; [B]Mee et al., 2004; [C]Green et al., 2004; [D]Turner et al., 1993; [E]Douglas et al., 1995.

4.4.3. Strontium concentrations for the surficial deposits of the upper SE

As with the cave sediments, the concentration of strontium (ppm) for the surficial deposits located around the Naracoorte region also increases with increasing silt content. The RBEs at Coonawarra and Padthaway have strontium concentrations that are comparable to the caves; however, at both sites, strontium concentrations are much lower in the sandy A horizons (10–20 ppm) compared to the clay-rich B horizons (20–40 ppm). The silt-dominated Bool Lagoon lunettes have strontium concentrations (40–76 ppm) and are more akin to the sandy silt horizons in the cave deposits rather than those dominated by sand.

The surficial sand units of the Naracoorte region have generally lower Sr concentrations than what is observed for the reddish and brown sandy silts, and the RBEs and lunette deposits. The concentration of strontium in the Bridgewater Formation is very low (3 ppm), while the modern beach sand from Robe (17 ppm) and the podsolic sand from the Robertson Cave entrance (18 ppm) are similar to those evident for the sand horizons in the caves. Strontium concentrations for deposits from the Lower Murray and the Coorong are higher than these sand units and increase with increasing silt content. The sand-rich river bank deposits near the ferry crossing at Wellington have strontium concentrations of 23 and 33.9 ppm, respectively. The Woods Well sandy silt exhibited a similar strontium concentration (25 ppm) to the sands from the Wellington area. The two more silt-rich deposits located in the low lying floodplain areas at the northern (Meningie; 78 ppm) and southern (Kingston; 82 ppm) ends of the Coorong have much higher strontium concentrations, corresponding to the organic matter rich silty cave horizons, the RBE clay horizons and the region's silt-laden lunettes.

5. Discussion

Previous sedimentary investigations in the Naracoorte Caves have led researchers to suggest that the

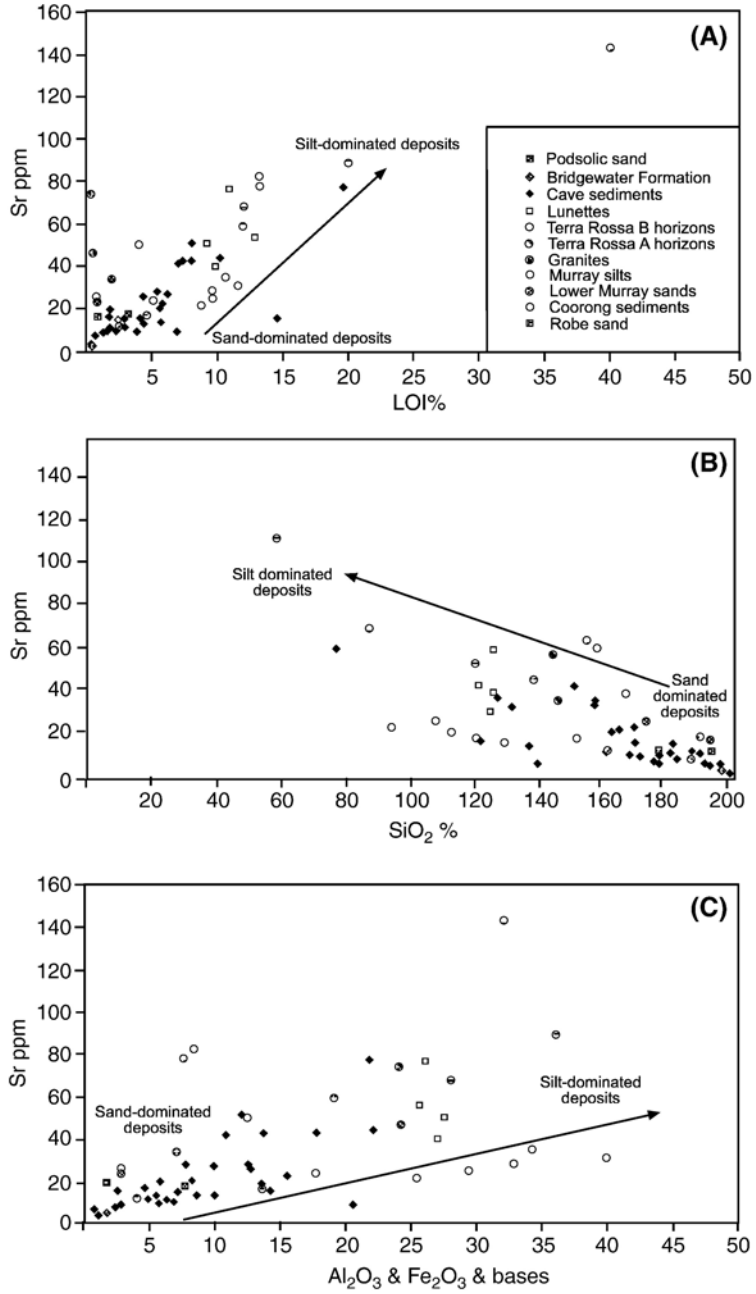

Fig. 10. (A) LOI vs. Sr; (B) SiO_2 vs. Sr, and (C) Sr vs. Al_2O_3/Fe_2O_3/bases for cave sediments and surficial deposits.

majority of the cave fills are eroded remnants of the regional surficial sand, silt, and clay deposits. Particular links have been made between the cave system's sand-dominated horizons and surficial dune deposits, such as the Bridgewater Formation and the Podsolic and Parilla sands (Wells et al., 1984; Moriarty et al., 2000); while the reddish sandy silt horizons have been directly related to the region's RBEs, and the podsolic sands are linked to the brown organic rich sandy silts (Moriarty et al., 2000; McDowell, 2001). Further physical characterisations, combined with mineralogical (XRD) and bulk sediment geochemical (XRF) analyses and $^{87}Sr/^{86}Sr$ isotopic analysis of the cave sediments presented here not only substantiate these relationships but also provide further insight into the true origins of much of the clastic sediments of the Naracoorte region.

Grain size distributions for the various cave sediment horizons from Robertson, Wet, Blanche, and Victoria Caves identify a distinct bimodal composition of medium to fine sands and coarse to medium silts. Thin section analysis indicates that quartz, with lesser, varying amounts of organic materials (i.e., charcoal) and silt aggregates are the dominant constituents of the cave sediments. Mineralogical analysis (XRD) supports these findings identifying significant quantities of quartz, clay minerals (smectite and kaolinite), and iron oxides (goethite). Bulk sediment geochemistry (XRF) recognises significant amounts of SiO_2, Al_2O_3, and Fe_2O_3, which correlates with the mineralogical data. LOI is also considerable in many sedimentary horizons, particularly in the brown sandy silts, and is more than likely a reflection of their significant organic matter content. Minimal variation in the $^{87}Sr/^{86}Sr$ ratios of the cave sediments is apparent, with the vast majority having values ranging from 0.720 to 0.725. This suggests that there has not been any significant alteration in the source of the strontium entering the cave system since sedimentation occurred in the main fossil chamber in Victoria Cave some 400 ka ago. Concentrations of strontium (ppm) in the cave sediment horizons increase corresponding to increasing silt fraction; however, apparent is little correlation between the strontium concentrations and $^{87}Sr/^{86}Sr$ ratios ($R^2=0.0021$). This suggests that the strontium in the cave sediments is almost entirely part of the silt to clay fraction and that it has been well mixed during transportation from its original source.

The geochemical and mineralogical characteristics of the upper SE's RBE's A and B horizons and the lunette deposits reveal many similarities to those identified for the cave sediments. They, like the cave sediments, are comprised of various combinations of quartz, clay minerals, and iron oxides and, accordingly, high SiO_2, Al_2O_3, and Fe_2O_3 contents. However, differences do exist between these deposits and the cave sediments; in particular, the distinct lack of illite evident in all cave sediments, while the Bool Lagoon lunettes and the RBE B horizons of the Padthaway region contain up to 20%. The apparent lack of illite in the cave sediments may be an artefact of analysis, with the smectite component being over-represented at the expense of illite, with this problem being encountered in similar studies of cave sediments (Knapp et al., 2004). But, the lack of illite is noticeable in many other surficial samples in the Coonawarra and Naracoorte area: in particular, the RBE's B horizons. This combined with the finer grain size exhibited by the Bool Lagoon lunette sediments suggests that the lack of illite is not an analytical error; rather, the smectite and kaolinite in the cave sediments have originated from the medium silt-sized RBEs of the Naracoorte and Coonawarra areas that are proximal to cave entrances. Hence, the finer lunette deposits and the Padthaway RBEs have had minimal direct input to cave sediment composition.

In comparison to these clay- and silt-rich deposits, the various sand-dominated facies of the upper SE's regressional dune system consist almost entirely of carbonates and quartz. Carbonate minerals (calcite, aragonite, Mg-calcite, ankerite, and dolomite) have been shown to predominate in the region's many aeolinite deposits, including modern dunes, relict dunes, and lagoonal facies (e.g., von der Borch, 1965; Gostin et al., 1988; Belperio, 1995; Wright and Wacey, 2005). Many of these facies also contain high amounts of bioclastic material (Murray-Wallace and Belperio, 1991). The carbonates that are present in the sediments at the present coast (Coorong and at Robe) are more easily weathered and are more indicative of the high and almost active biotic component that exists there (Belperio, 1995). In comparison, the older Pleistocene-aged Bridgewater Formation is almost entirely quartz and calcite, which are more resistant to weathering and alteration. While quartz is present in large quantities in the cave sediments; carbonates, with the exception of the calcite evident in Blanche Cave are none existent. The absence of carbonate minerals from many of the cave sediments can be attributed to a combination of two factors, firstly significant weathering and destruction resulting from aeolian transportation to the cave area, then the effects of dissolution within the cave system itself.

Comparison of the cave sediment's $^{87}Sr/^{86}Sr$ ratios with the regional surficial deposits allows for further insight into the origin of these sediments. A significant correlation between the cave sediments and the Holocene age podsolic sands located near Robertson Cave (0.724, $n=1$), the sandy A horizons of the Coonawarra RBEs (0.727; $n=5$), the modern beach sand from Robe (0.725, $n=1$), and the finer grained silty lunette deposits from Bool Lagoon (0.722; $n=4$). $^{87}Sr/^{86}Sr$ ratios for the sandy A horizon of RBEs located to the north at Padthaway, the RBEs B horizons from both Coonawarra (0.718; $n=13$) and Padthaway (0.715; $n=6$), and the coarse shell-laden Bridgewater Formation (0.744) do not correlate as well. Thus, the surficial deposits proximal to the cave area, such as the Coonawarra's RBE's A horizons and the podsolic sands (both of medium grain size and consisting of higher amounts of quartz), are most closely related to the cave sediments, while mineralogical and grain size differences discount any

significant contribution from the Bool Lagoon lunette materials and the modern dune sands of the Robe area. Furthermore, the narrow range of $^{87}Sr/^{86}Sr$ ratios of the cave sediments suggests that a large portion of the strontium-dominated silt present in the SE may well have been derived from a similar source.

The clear physical and geochemical similarities that have been identified between the cave sediments and many of the local surficial units of the Naracoorte region mean that they are undoubtedly linked. Yet to say that the cave sediments have been derived from these local deposits is paradoxical, primarily because of the fact that many of the cave sediments are possibly older or of similar age to that estimated for some of the surficial deposits. For instance, the cave sediments investigated in Victoria Cave are thought to be 400 ka BP (Ayliffe and Veeh, 1988), whereas the RBEs from Coonawarra are thought to have developed over the last 100 ka (Mee et al., 2004; Krull et al., 2006). This age overlap (combined with the close sedimentological, geochemical, isotopic, and mineralogical characteristics exhibited between surficial and cave sediments) suggests that while many of the cave deposits are directly linked to the surface deposits, they have probably all originated from a similar source and possibly evolved during a similar time period.

Investigations into the origins and development of the Coonawarra RBEs have been documented (Mee et al., 2004; Krull et al., 2006). Mee et al. (2004) compared $^{87}Sr/^{86}Sr$ ratios and Ti/Zr ratios of the RBE's A and B soil horizons and the underlying calcareous bedrock and concluded that material of aeolian origin contributed significantly to their formation rather than dissolution of the underlying limestone. This was further supported by ^{14}C age determinations for the A and B horizons undertaken by Krull et al. (2006). Mee et al. (2004) discussed the sources of this aeolian material, suggesting that much of it may have been derived from the shales associated with the Adelaide geosyncline transported to the Naracoorte region by the prevailing westerly wind regime. Correlation of average $^{87}Sr/^{86}Sr$ ratios for the Kanmantoo shales located on Kangaroo Island (0.716) and the Fleurieu Peninsula (0.725) with the RBEs and, as such, the cave sediments (0.72) supported this argument. However, unlike the consistency in the $^{87}Sr/^{86}Sr$ evident for the cave and surficial deposits of the Naracoorte area, the Kanmantoo Shale Group exhibits significant variation. It is anticipated that if these units were a significant source of detritus to the Naracoorte area then the isotopic variation that exists within the group would also be apparent in the cave and surficial deposits of the Naracoorte area, which is not the case. Furthermore, other units that comprise the Adelaide geosyncline, such as the Adelaidean Group, would also have contributed detritus to the area. $^{87}Sr/^{86}Sr$ ratios for the Adelaidean are generally much higher and also more varied (0.72–0.84; Turner et al., 1993) than those evident for the surficial units and cave sediments of the Naracoorte region (Fig. 9). Therefore, the units from the Adelaide geosyncline are unlikely to have contributed major amounts of silt material to the deposits of the Naracoorte area.

The granitic and basaltic deposits that are scattered throughout the SE region are also a possible source of the silt-sized sedimentary material now found around Naracoorte. To the north and west of Naracoorte are numerous small outcrops of Palaeozoic granites, while in the lower SE around Mt. Gambier many basalt deposits associated with Quaternary volcanic centres exist. Soils formed from the weathered products of both these deposits (Blackburn et al., 1965). In the immediate vicinity of Mt. Monster (near Keith), soils appear to have been partially derived from granite (Blackburn et al., 1965), while a number of soils around Mt. Shank and Mt. Gambier formed from the weathered components of basalt (Sheard, 1978, 1983). In both instances, the soils in question are restricted close to their source and are not present in the Naracoorte area. Variation between the $^{87}Sr/^{86}Sr$ ratios for the lower SE basalts (0.703–0.705; Price et al., 1997), the granite outcrop of Mt. Monster (0.7840), and the sediments of the Naracoorte area suggests that these two units have not contributed in any significant manner to the latter's formation. This is further supported by a lack of feldspars (granite) and by pyroxenes and olivines (basaltic soils) present in the cave sediments or, for that matter, in any of the major surficial facies proximal to the Naracoorte Caves.

Another possible source of clastic material to the Naracoorte region is the aeolian active interior of Australia. Fluxes of sediments from this region could have occurred, particularly during periods of dry and windy conditions like those experienced during past glacial peaks when wind regimes were thought to be more predominantly from the north to northwest (Bowler et al., 1976; White, 1994; Hesse and McTainsh, 2003). However, many noncarbonate sedimentary units in central Australia exhibit $^{87}Sr/^{86}Sr$ ratios in excess of 0.8 (eg. Harrington and Herczeg, 2003). Also, most dust from the large interior arid areas is deposited within several hundred kilometres of its origin and is thus retained within the central Australian drainage network (McTainsh, 1984). This suggests that

the sediments from arid-central Australia are unlikely to have contributed any major amounts of material directly to the Naracoorte region.

The fact that the SE region not only consists of the Gambier Embayment but also incorporates the lower part of the Murray Basin (Alderman, 1973) means that sediments in the SE region may have originated from the Murray–Darling hydrologic system. This interaction is supported by mineralogical analysis of sediments from the coastal shelf off the southern coast of Kangaroo Island, which compare favourably with the mineralogy evident for the Murray and Darling tributaries (Gingele and De Deckker, 2004; Gingele et al., 2004). Apparent in the coastal shelf sediments were significant amounts of smectite, illite, and kaolinite and minor amounts of chlorite, which were all observed in large amounts in various parts of the Murray–Darling Basin. This clay mineralogy for the coastal shelf sediments and the Murray–Darling basin also correlates with that observed for the cave sediments and the surficial deposits of the Naracoorte area.

$^{87}Sr/^{86}Sr$ isotope data for the sediments of the Murray–Darling Basin further strengthens its role as a source of sediment to the Naracoorte area. Suspended particulate matter (SPM) from the lower Murray system sees results of between 0.71–0.72 for the various silt size fractions (Douglas et al., 1995, 1999). These correlate strongly with $^{87}Sr/^{86}Sr$ isotope results for the cave sediments, Bool Lagoon lunettes, RBE A horizons, and Coorong sediments (Fig. 9). This suggests that the finer grain silts of the Murray Basin were a vital contributor of silt and clay material to many of the deposits that are evident in the SE today, including the cave sediments. Relationships between silt content, LOI, strontium concentrations, SiO_2, Al_2O_3, Fe_2O_3, and base cation contents further support this interpretation (Fig. 10). High silt content correlates with high LOI and Sr and with low SiO_2 contents, while Al_2O_3, Fe_2O_3, and base cation content increase with increasing Sr. This suggests that much of the Sr now present in the deposits of the SE is part of the clay mineral bearing silt component. The fact that this Sr exhibits quite a uniform presence throughout the silt-dominated deposits of the region and the cave sediments implies that it has come from a single source (the Murray River) and has subsequently been transported and incorporated into the finer components of the SE sedimentary system.

6. Conclusions

Geochemical, mineralogical, and $^{87}Sr/^{86}Sr$ isotope ratio data suggest that the Naracoorte Cave sediments, as well as many surficial deposits of the upper SE have been derived from silts and clays originating from the Murray–Darling Basin that have mixed with the regions sand units. The uniform $^{87}Sr/^{86}Sr$ ratios evident for many of the Naracoorte Cave and surficial sediments indicates that the fine-grained component of this mud—with its high organic matter content, relatively high base cation concentrations, and low $^{87}Sr/^{86}Sr$ ratios (Douglas et al., 1995)—appears to have overwhelmed other dust sources, resulting in a homogenisation of the geochemical signature of fine-grained soil solids in the area. Aeolian and hydrological transport removed this material from the lower reaches of the Murray River and allowed it to then be heterogeneously mixed with regional coastal sands and carbonates. Regional tectonic and climatic events combined with soil processes, such as clay illuviation, to shape and mould these sediments into the geomorphological features that we see today. During this geomorphological evolution, erosion of surficial deposits proximal to the individual cave entrances allowed for them to accumulate and develop their own unique sedimentary record while keeping the homogeneous geochemical traits that many of the sediments of the region possess.

Acknowledgements

We would like to thank the Department of Environment and Heritage (DEH) for funding the study. Dr. John Foden and Mr. David Bruce at Mawson Laboratories, University of Adelaide, for strontium analysis, Mr. John Stanley also at Mawson Laboratories, University of Adelaide, for XRF analysis. Mr. Mark Raven, CSIRO Land and Water, for XRD analysis. Mr. Steve Bourne and Dr. Liz Reed at Naracoorte Caves regarding field work logistics and cave access.

References

Alderman, A.R., 1973. Southern Aspect, An Introductory View of South Australian Geology. South Australian Museum, Adelaide. 158 pp.

Ayalon, A., Bar-Matthews, M., Kaufman, A., 1999. Petrography, strontium, barium and uranium concentrations, and strontium and uranium isotope ratios in speleothems as palaeoclimatic proxies: Soreq Cave, Israel. The Holocene 9 (6), 715–722.

Ayliffe, L.K., Veeh, H.H., 1988. Uranium-series dating of speleothems and bones from Victoria Cave, Naracoorte, South Australia. Chemical Geology 72, 211–234.

Ayliffe, L.K., Marinelli, P.C., Moriarty, K.C., Wells, R.T., McCulloch, M.T., Mortimer, G.E., Hellstrom, J.C., 1998. 500 Ka precipitation record from southeastern Australia: evidence for interglacial aridity. Geology 26, 147–150.

Belperio, A.P., 1995. Quaternary. In: Drexel, J.F., Preiss, W.V. (Eds.), The Geology of South Australia, The Phanerozoic. Chapter 11. Vol. 2. Bulletin 54, Geology survey of South Australia, Adelaide, pp. 219–280.

Blackburn, G., Bond, R.D., Clarke, A.R.P., 1965. Soil development associated with stranded beach ridges in south-east South Australia. Soil Publication 22. CSIRO, Melbourne. 65 pp.

Bowler, J.M., Hope, G.S., Jennings, J.N., Singh, G., Walker, D., 1976. Late Quaternary climates of Australia and New Guinea. Quaternary Research 6, 359–394.

Brown, S.P., Wells, R.T., 2000. A middle Pleistocene vertebrate fossil assemblage from Cathedral Cave, Naracoorte, South Australia. Transactions of the Royal Society of South Australia 124 (2), 91–104.

Capo, R.C., Stewart, B.W., Chadwick, O.A., 1998. Sr Isotopes as tracers of ecosystem processes: theory and methods. Geoderma 82 (1–3), 197–225.

Cook, P.J., Colwell, J.B., Firman, J.M., Lindsay, J.M., Schwebel, D.A., Von Der Borch, C.C., 1977. The late Cainozoic sequence of southeast South Australia and Pleistocene sea-level changes. BMR Journal of Australian Geology and Geophysics 2, 81–88.

Cooke, M.J., Stern, L.A., Banner, J.L., Mack, L.E., Stafford Jr., T.W., Toomey III, R.S., 2003. Precise timing and rate of massive late Quaternary soil denudation. Geology 31, 853–856.

Craft, C.B., Seneca, E.D., Broome, S.W., 1991. Loss on ignition and Kjeldahl digestion for estimating organic carbon and total nitrogen in estuarine marsh soils: calibration and dry combustion. Estuaries 14 (2), 175–179.

Desmarchelier, J.M., Goede, A., Ayliffe, L.K., McCulloch, M.T., Moriarty, K., 2000. Stable isotope record and its palaeoenvironmental interpretation for a late Middle Pleistocene speleothem from Victoria Fossil Cave, Naracoorte, South Australia. Quaternary Science Reviews 19, 763–774.

Dickson, B.L., Scott, K.M., 1998. Recognition of aeolian soils of Blayney District, N.S.W.: implications for mineral exploration. Journal of Geochemical Exploration 63, 237–251.

Dogramaci, S.S., Herczeg, A.L., 2002. Strontium and carbon isotope constraints on carbonate-solution interactions and inter-aquifer mixing in groundwaters of the semi-arid Murray Basin, Australia. Journal of Hydrology 262, 50–67.

Douglas, G.B, Gray, C.M, Hart, B.T., Beckett, R., 1995. A strontium isotopic investigation of the origin of suspended particulate matter (SPM) in the Murray–Darling River system, Australia. Geochimica et Cosmochimica Acta 59 (18), 3799–3815.

Douglas, G.B., Hart, B.T., Beckett, R., Gray, C.M, Oliver, R.L., 1999. Geochemistry of Suspended Particulate Matter (SPM) in the Murray–Darling river system: a conceptual isotopic/geochemical model for the fractionation of major, trace and rare earth elements. Aquatic Geochemistry 5, 167–194.

Faure, G., Powell, J.L., 1972. Strontium Isotope Geology. Springer-Verlag, New York. 188 pp.

Fitzpatrick, R.W., Chittleborough, D.J., 2002. Titanium and zirconium minerals. Soil mineralogy with environmental applications. Soil Science of America Book Series, vol. 7. 667–690 pp.

Forbes, M.S., Bestland E.A., in press. Guano-derived deposits within the sandy cave fills of Naracoorte, South Australia. Alcheringa.

Forbes, M.S., Bestland E.A., Wells, R.T., Krull E.S., in press. Palaeoenvironmental reconstruction of the Late Pleistocene to Early Holocene Robertson Cave sedimentary deposit, Naracoorte, South Australia. Australian Journal of Earth Sciences.

Ford, D.C., Williams, P.W., 1989. Karst Geomorphology and Hydrology. Unwin Hyman Publishing, London. 604 pp.

Frumkin, A., Stein, M., 2004. The Sahara-East Mediterranean dust and climate connection revealed by strontium and uranium isotopes in a Jerusalem speleothem. Earth and Planetary Science Letters 217 (3–4), 451–464.

Gingele, F.X., De Deckker, P., 2004. Finger printing Australia's rivers with clay minerals and the application for the marine record of climate change. Australian Journal of Earth Sciences 51, 339–348.

Gingele, F.X., De Deckker, P., Hillenbrand, C-D., 2004. Late Quaternary terrigenous sediments from the Murray Canyons area, offshore South Australia and their implications for sea level change, palaeoclimate and palaeodrainage of the Murray–Darling Basin. Marine Geology 212 (1–4), 183–197.

Goede, A., McCulloch, M., McDermott, M., Hawkesworth, F., 1998. Aeolian contribution to strontium and strontium isotope variations in a Tasmanian speleothem. Chemical Geology 149 (1–2), 37–50.

Gostin, V.A., Belperio, A.P., Cann, J.H., 1988. The Holocene non-tropical coastal and shelf carbonate provenance of South Australia. Sedimentary Geology 60, 51–70.

Green, G.P., Bestland, E.A., Walker, G.S., 2004. Distinguishing sources of base cations in irrigated and natural soils: evidence from strontium isotopes. Biogeochemistry 68 (2), 199–225.

Grün, R., Moriarty, K.C., Wells, R.T., 2001. ESR dating of the fossil deposits in the Naracoorte Caves, South Australia. Journal of Quaternary Science 16, 49–59.

Harrington, G.A., Herczeg, A.L., 2003. The importance of silicate weathering of a sedimentary aquifer in arid central Australia by very high $^{87}Sr/^{86}Sr$ ratios. Chemical Geology 199, 281–292.

Hesse, P.P., McTainsh, G.H., 2003. Australian dust deposits: modern processes and the Quaternary record. Quaternary Science Reviews 22, 2007–2035.

Hill, C., Forti, P., 1997. Cave Minerals of the World. National Speleological Society Inc, Huntsville. 463 pp.

Hosking, J.S., Neilson, M.E., Carthew, A.R., 1957. A study of clay mineralogy and particle size. Australian Journal of Agricultural Research 8 (1), 45–74.

Karkanas, P., Kyparissi-Apostalika, N., Bar-Yosef, O., Weiner, S., 1999. Mineral assemblages in Theopetra, Greece: a framework for understanding diagenesis in a prehistoric cave. Journal of Archaeological Science 26, 1171–1180.

Knapp, E.P., Terry, D.O., Harbor, D.J., Thren, R.C., 2004. Reading Virginias paleoclimate from the geochemistry and sedimentology of clastic sediments. In: Sasowsky, I.D., Mylroie, J. (Eds.), Studies of Cave Sediments Physical and Chemical Records of Paleoclimate. Kluwer Academic /Plenum Publishers, New York, p. 329.

Krull, E.S., Bestland, E.A., Skjemstad, J.O., Parr, J.F., 2006. Organic geochemistry ($\delta^{13}C$, $\delta^{15}N$, 13C-NMR) and age determinations (14C and OSL) of Red–Brown Earths from the Coonawarra–Padthaway region of South Australia: implications for soil genesis. Geoderma 132 (3–4), 344–360.

McDowell, M.C., 2001. Fossil faunas of Robertson and Wet Cave. M.S. Thesis, Flinders University of South Australia, Adelaide.

McTainsh, G., 1984. Dust processes in Australia and West Africa: a comparison. Search 16, 104–106.

Mee, A.J., Bestland, E.A., Spooner, N.J., 2004. The age and origin of terra rossa soils in the Coonawarra area of South Australia. Geomorphology 58, 1–25.

Moriarty, K.C., McCulloch, M.T., Wells, R.T., McDowell, M.C., 2000. Mid-Pleistocene cave fills, megafaunal remains and climate change at Naracoorte, South Australia: towards a predictive model using U/Th dating of speleothems. Palaeogeography, Palaeoclimatology, Palaeoecology 159, 113–143.

Murray-Wallace, C.V., Belperio, A.P., 1991. The last interglacial shoreline in Australia—a review. Quaternary Science Review 10 (5), 411–461.

Norrish, K., Chappell, B.W., 1977. X-ray fluorescence spectrometry, In: Zussman, J. (Ed.), Physical Methods in Determinative Mineralogy, 2nd ed. Academic Press, pp. 201–272.

Norrish, K., Rogers, L.E.R., 1956. The mineralogy of some terra rossa and rendzinas of South Australia. Journal of Soil Science 7, 294–301.

Pate, F.D., McDowell, M.C., Wells, R.T., Smith, A.M., 2002. Last recorded evidence for megafauna at Wet Cave Naracoorte, South Australia 45000 years ago. Australian Archaeology 54, 53.

Price, R.C., Gray, C.M., Frey, F.A., 1997. Strontium isotopic and trace element heterogeneity in the plains basalts of the newer volcanic province, Victoria, Australia. Geochimica et Cosmochimica Acta 61 (1), 171–192.

Quade, J., Chivas, A.R., McCulloch, M.T., 1995. Strontium and carbon isotope tracers and the origins of soil carbonate in South Australia and Victoria. Palaeogeography, Palaeoclimatology, Palaeoclimatology 113, 103–117.

Reed, E.H., 2002. Vertebrate taphonomy of large mammal bone deposits, Naracoorte Caves World Heritage Area. Ph.D. Dissertation, The Flinders University of South Australia, Adelaide.

Shahack-Gross, R., Berna, F., Karkanas, P., Weiner, S., 2004. Bat Guano and preservation of archaeological remains in cave sites. Journal of Archaeological Science 31, 1259–1272.

Sheard, M.J., 1978. Geological history of the Mt Gambier volcanic complex, southeast South Australia. Transactions of Royal Society of South Australia 102, 125–139.

Sheard, M.J., 1983. Volcanoes of the Mt Gambier area. Mineral Information Series, vol. 12. South Australian Department of Mines and Energy, Adelaide. 2 pp.

Sprigg, R.C., 1952. Sedimentation in the Adelaide geosyncline and the formation of the continental terrace. In: Glaessner, M.F., Rudd, E.A. (Eds.), Sir Douglas Mawson Anniversary Volume. University of Adelaide, Adelaide, pp. 153–159.

Sprigg, R.C., 1979. Stranded and submerged sea–beach systems of southeast South Australia and the aeolian desert cycle. Sedimentary Geology 22, 53–96.

Stace, H.C.T., Hubble, G.D., Brewer, R., Northcote, K.H., Sleeman, J.R., Mulcahy, M.J., Hallsworth, E.G., 1968. A Handbook of Australian Soils. Rellim, Adelaide. 283–287 pp.

Stewart, B.W., Capo, R.C., Chadwick, O.A., 1998. Quantitative strontium isotope models for weathering, pedogenesis and biogeochemical cycling. Geoderma 82 (1/3), 173–195.

Turner, S., Foden, J., Sandiford, M., Bruce, D., 1993. Sm–Nd evidence for provenance of sediments from the Adelaide fold belt and southeast Australia with implications for episodic crustal addition. Geochimica et Cosmochimica Acta 57, 1837–1856.

Twidale, C.R., Campbell, E.M., Bourne, J.A., 1983. Granite forms, karst and lunettes. In: Tyler, M.J., Twidale, C.R., Ling, J.K., Holmes, J.W. (Eds.), Natural History of South East. Royal Society of South Australia, Adelaide, pp. 25–37.

von der Borch, C.C., 1965. The distribution and preliminary geochemistry of modern carbonate sediments of the Coorong area, South Australia. Geochimica et Cosmochimica Acta 29, 781–799.

Wells, R.T., Moriarty, K., Williams, D.L.G., 1984. The fossil vertebrate deposits of Victoria Fossil Cave Naracoorte: an introduction to the geology and fauna. The Australian Zoologist 21, 305–333.

White, M.E., 1994. After the Greening: The Browning of Australia. Kangaroo Press, Roseville. 287 pp.

White, S.Q., 2005. Karst and landscape evolution in parts of the Gambier Karst Province, southeast South Australia and Western Victoria, Australia. Ph.D. Dissertation, La Trobe University, Victoria.

Wright, D.T., Wacey, D., 2005. Precipitation of dolomite using sulphate-reducing bacteria from the Coorong Region, South Australia: significance and implications. Sedimentology 52, 987–1008.

Zanin, Y.N., Tsykin, R.A., Dar'in, A.V., 2005. Phosphorites of the Arheologicicheskaya Cave (Khakassia, East Siberia). Lithology and Mineral Resources 40 (1), 48–55.